

1 **Modelling PM_{2.5} during severe atmospheric pollution episode in Lagos, Nigeria:**
2 **Spatiotemporal variations, source apportionment, and meteorological influences**

3
4 Ishaq Dimeji Sulaymon^{a*}, Yuanxun Zhang^{b,c}, Philip K. Hopke^{d,e}, Fei Ye^a, Kangjia Gong^a,
5 Jianjiong Mao^a, Jianlin Hu^{a*}

6
7 ^a Jiangsu Key Laboratory of Atmospheric Environment Monitoring and Pollution Control,
8 Collaborative Innovation Center of Atmospheric Environment and Equipment
9 Technology, School of Environmental Science and Engineering, Nanjing University of
10 Information Science & Technology, Nanjing, 210044, China

11 ^b College of Resources and Environment, University of Chinese Academy of Sciences,
12 Beijing 100049, China

13 ^c CAS Center for Excellence in Regional Atmospheric Environment, Chinese Academy of
14 Sciences, Xiamen, 361021, China

15 ^d Center for Air Resources Engineering and Science, Clarkson University, Potsdam, NY
16 13699, USA

17 ^e Department of Public Health Sciences, University of Rochester School of Medicine and
18 Dentistry, Rochester, NY 14642, USA

19 _____

20 * Corresponding author. E-mail address: sulaymondimeji@nuist.edu.cn; jianlinhu@nuist.edu.cn

21

22 **Key Points:**

- 23 • Lagos experienced a prolonged severe PM_{2.5} pollution episode in January 2021.
24 • PM_{2.5} pollution was enhanced by unfavorable meteorological conditions.
25 • Effective emissions control strategies to reduce PM_{2.5} concentrations are urgently
26 required in Lagos.

27

28

29

30

31

32

33

34

35

36

37 **Abstract**

38 In 2021, the World Health Organization (WHO) ranked Nigeria among the most
39 polluted nations in the world, an indication of a deteriorating air quality, especially in the
40 major urban areas of the country, which might pose adverse human health impacts. In this
41 study, the Integrated Source Apportionment Method (ISAM) tool in the Community
42 Multiscale Air Quality (CMAQ) model (CMAQ-ISAM) was employed to quantify the
43 contributions of eight emissions sectors to fine particulate matter (PM_{2.5}) and its major
44 components in Lagos during a prolonged severe atmospheric pollution episode (APE) in
45 January 2021. The influence of meteorological conditions on the formation and
46 dispersion of PM_{2.5} during the APE was also elucidated. Spatially, elevated PM_{2.5}
47 concentrations were found in the northwestern region of Lagos, an urban area with larger
48 anthropogenic emissions. Residential and industry were the two major sources of PM_{2.5}.
49 Residential contributed the most to total PM_{2.5} (~40 µg/m³), followed by industry (~20
50 µg/m³). High concentrations of secondary inorganic aerosols (SIA) at the northwest and
51 upper northern areas of Lagos were majorly attributed to residential and industry sectors.
52 In addition, sulfate accounted for the largest fraction of PM_{2.5}, with residential, industry,
53 and energy being its major sources. Residential, industry, and on-road sectors dominated
54 the contributions to nitrate, while residential and industry were the major contributors to
55 ammonium. Furthermore, the elevated PM_{2.5} concentrations during the APE were greatly
56 enhanced by unfavorable meteorological conditions. This study provides insights for
57 designing effective emissions control strategies to mitigate future severe PM_{2.5} pollution
58 episode in Lagos.

59 **Keywords:** Fine particulate matter; Source apportionment; CMAQ-ISAM; Atmospheric
60 pollution episode; Residential emissions; Meteorological influences.

61 **1. Introduction**

62 Due to rapid population growth, accelerated urbanization, economic advancement,
63 and fast industrialization, Nigeria has been suffering from severe air pollution for more
64 than two decades (Abiye et al., 2013, 2014; Owoade et al., 2013; Sulaymon et al., 2020).
65 In 2021, the WHO ranked Nigeria among the most polluted nations in the world (WHO,
66 2021), making it a great concern for the Nigerian air quality experts. The anthropogenic
67 and natural emissions are the major sources of particulate matter and gaseous primary air
68 pollutants (Owoade et al., 2013). Air pollution is largely linked to emissions from
69 anthropogenic activities (either local or regional) (Sulaymon et al., 2020, 2021a) and
70 aggravated by unfavorable meteorological factors (Hua et al., 2021; Hu et al., 2016;
71 Sulaymon et al., 2021a, 2021b). Severe air pollution is strongly correlated with visibility
72 reductions (Jiang et al., 2021; Li et al., 2019; Wang et al., 2018), changes in ecosystem
73 services, effects on climate (Jiang et al., 2021; Zhao et al., 2021), acid rain (Owoade et al.,
74 2021), and very serious human health impacts (Croft et al., 2019; Hopke et al., 2019;
75 Shen et al., 2020; Yan et al., 2018), such as pneumonia, acute respiratory disorders,
76 breathing problems, and chronic asthma (Rizwan et al., 2013). The global burden of
77 disease project (GDB, 2020) has estimated that about 4.2 million premature deaths per
78 annum around the globe are the result of exposure to air pollution.

79 Meteorological factors play major roles in the formation, accumulation, and
80 dispersion of air pollutants (Hu et al., 2016; Islam et al., 2015; Mao et al., 2022; Okimiji
81 et al., 2021; Owoade et al., 2021; Sulaymon et al., 2021a, 2021b, 2021c). Previous
82 studies have posited that the atmospheric pollution dispersion is greatly influenced by
83 relative humidity (RH), wind speed (WS), and planetary boundary layer height (PBLH)

84 (Li et al., 2019; Liu et al., 2017; Zhang et al., 2019; Zhang et al., 2018), and that low WS
85 and PBLH hinder atmospheric pollutant dispersion and consequently lead to severe air
86 pollution episodes (Dai et al., 2020; Li et al., 2019; Liu et al., 2017; Sulaymon et al.,
87 2021a; Wang et al., 2020; Zhang et al., 2019).

88 Prior to January 2021, there were no ambient air quality monitoring networks in
89 any of Nigerian cities. The lack of ambient data meant that the temporal and spatial
90 variations of the major air pollutants (gaseous pollutants and particulate matter and its
91 components) were unknown. Thus, studies to investigate the air quality and support
92 development of effective pollution control strategies and reduce associated human health
93 risks were very limited (Kitagawa et al., 2022; Hu et al., 2016). However, the problems
94 associated with the air quality assessment in countries/regions with no or limited
95 monitoring networks could be overcome through the use of source-tracking chemical
96 transport models (CTMs) (Kitagawa et al., 2022). CTMs can simulate air pollutants with
97 high resolution of temporal and spatial distributions (Kota et al., 2018), give hourly
98 averaged gridded concentrations (Kitagawa et al., 2022), be used for source
99 apportionment studies (Appel et al., 2020; Li et al., 2021; Ma et al., 2021; Shi et al.,
100 2017), employed in human exposure assessment to air pollution (Guo et al., 2019; Reis et
101 al., 2018), as well as utilized in epidemiological studies to unravel the adverse effects of
102 air pollution on population (Andreão et al., 2020). CTMs have been extensively used in
103 many parts of the world, such as North America (Guo et al., 2018; Hu et al., 2015a; Pan
104 et al., 2017; Ying and Kleeman, 2006; Wang et al., 2021a; Ying et al., 2015; Zhang et al.,
105 2013, 2014), China (Hu et al., 2015b, 2016, 2017; Gong et al., 2021; Ma et al., 2021;
106 Qiao et al., 2015, 2019; Sulaymon et al., 2021a, 2021b; Wang et al., 2020; Ying et al.,

107 2014), India (Guo et al., 2017, 2019; Guttikunda and Jawahar, 2014; Kota et al., 2014,
108 2018; Marrapu et al., 2014; Ye et al., 2022), South America (Albuquerque et al., 2018,
109 2019; Kitagawa et al., 2021, 2022; Nedbor-Gross et al., 2018; Pedruzzi et al., 2019, 2022),
110 and Africa (Kumar et al., 2022; Marais et al., 2014, 2019).

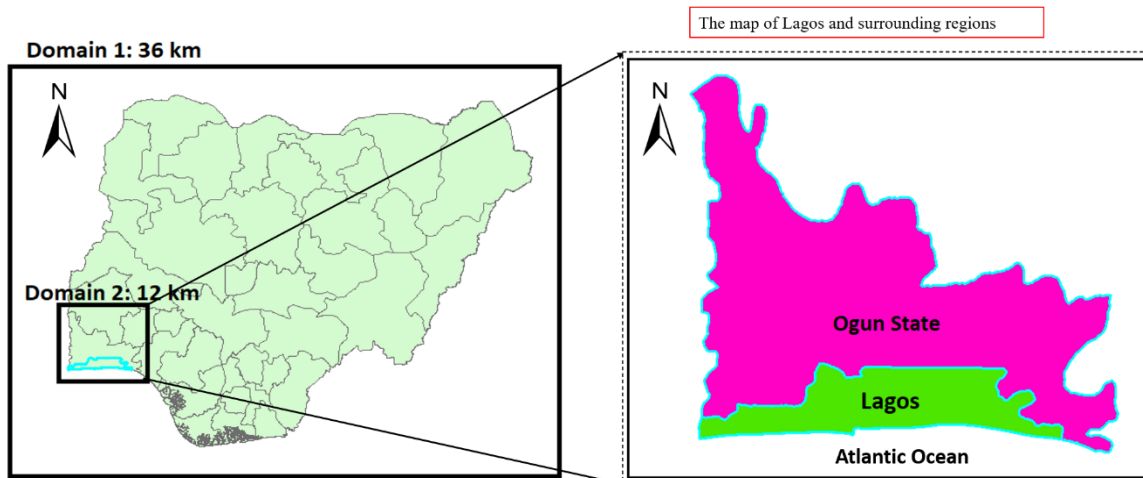
111 With a population of about 23.5 million as at 2018, Lagos is the largest
112 metropolitan city in Africa, and also the most economically and industrially-developed
113 city in Nigeria. As a result, the city has been suffering from severe fine particulate matter
114 ($PM_{2.5}$) pollution for more than two decades. To design effective emissions control
115 strategies towards abating $PM_{2.5}$ pollution in any region, it is imperative to elucidate the
116 contributions of various emissions sectors to $PM_{2.5}$ and its major components, as well as
117 the meteorological influences over the region. The present work represents the first study
118 that utilized the source-tracking Community Multiscale Air Quality (CMAQ) model to
119 quantify the contributions of different emissions sectors to $PM_{2.5}$ and its major
120 compositions in Lagos during a prolonged severe atmospheric pollution episode (APE) in
121 January 2021. The capability and fidelity of the CMAQ model in simulating $PM_{2.5}$ in
122 Lagos was validated by comparing the predicted concentrations with observation data,
123 and the spatiotemporal distributions of $PM_{2.5}$ during the APE period were analyzed. In
124 addition, the impacts of meteorological conditions on $PM_{2.5}$ during the APE were
125 elucidated. This study provides insights into the emissions sectors dominating $PM_{2.5}$
126 pollution in Lagos and the meteorological influences, and the results could serve as
127 scientific basis for formulating cost-effective emissions control strategies towards
128 mitigating $PM_{2.5}$ pollution in Lagos and the surrounding regions.

129

130 **2. Methodology**

131 *2.1. Model configurations*

132 The Community Multiscale Air Quality version 5.3.2 (CMAQv5.3.2) model was
133 employed to simulate the air quality in Lagos, Nigeria. The required meteorological fields
134 for the CMAQ model were simulated using the Weather Research and Forecasting (WRF)
135 model version 4.0. The initial and boundary conditions (IC/BC) of WRF model were
136 based on the dataset of NCEP FNL (Final) Operational Model Global Tropospheric
137 Analysis. The major physics schemes are listed in Table S1. Further detailed settings and
138 configurations of WRF model adopted in this study can be found in previous studies (Hu
139 et al., 2015b, 2016; Wang et al., 2021b). In this study, the simulations were conducted in
140 two domains using one-way nesting approach (Fig. 1). Domain 1 covers the entire
141 Nigeria with a horizontal resolution of 36 km x 36 km (137 x 107 grids). Domain 2
142 mostly covers Lagos and surrounding areas at with a horizontal resolution of 12 km x 12
143 km (127 x 202 grids). The model was configured with the State-wide Air Pollution
144 Research Center version 07 (SAPRC07tic) photochemical mechanism and the AERO6i
145 aerosol module (Sulaymon et al., 2021a, 2021b). Details about the vertical resolution of
146 the two CMAQ domains have been described in Sulaymon et al. (2021b). The simulation
147 period was January 2021, during which two severe APEs occurred. The IC/BC of
148 Domain 1 simulation were generated using the default profiles provided by the CMAQ
149 model. The IC/BC used for the 12 km domain simulation were estimated based on the
150 results of the nested simulation. To minimize the effects of initial conditions on the
151 model predictions, the simulation started five days ahead of the simulation period, hence,
152 regarded as the spin-up period (Tao et al., 2020).



153

154 **Fig. 1.** The WRF-CMAQ simulation domains used in this study (left) and the map of
 155 Lagos and surrounding regions (right).

156

157 2.2. *Emissions inventory*

158 In this study, the Integrated Source Apportionment Model (ISAM), a source
 159 tracking tool in the CMAQ model, was applied to quantify the source contributions to
 160 PM_{2.5} and its major components (Jiang et al., 2021; Kwok et al., 2013; Li et al., 2021) in
 161 Lagos. The anthropogenic emissions used in this study were derived from the Emissions
 162 Database for Global Atmospheric Research version 5.0 (EDGARv5.0) (Crippa et al.,
 163 2020). The EDGAR emissions inventory includes the annual emissions of carbon
 164 monoxide (CO), nitrogen oxides (NO_x), sulfur dioxide (SO₂), ammonia (NH₃), non-
 165 methane volatile organic compounds (NMVOCs), PM_{2.5}, particulate matter with an
 166 aerodynamic diameter less than 10 μm (PM₁₀), elemental carbon (EC), and organic
 167 carbon (OC) from various emissions sectors and with a spatial resolution of 0.1° x 0.1°.
 168 The emissions sectors were subsequently classified into six categories (agriculture,
 169 residential, industry, energy, on-road transportation, and off-road transportation). It is
 170 worthy to mention that the EDGAR emissions inventory had been used in numerous
 171 previous studies in India (Guo et al., 2019, 2018, 2017; Kota et al., 2018), China (Qiao et

172 al., 2019), and Africa as a continent (Kumar et al., 2022; Mazzeo et al., 2022). In addition,
173 biogenic emissions were estimated with the Model of Emissions of Gases and Aerosols
174 from Nature (MEGAN) version 2.1 (Guenther et al., 2012). Also, open burning emissions
175 were generated based on the data obtained from the Fire Inventory from NCAR (FINN)
176 (Wiedinmyer et al., 2011). Furthermore, sea salt and windblown emissions were
177 generated inline (Sulaymon et al., 2021a, 2021b). Overall, a total of eight emission
178 sectors were tracked in the ISAM model. Further details regarding the emission
179 processing can be found in Qiao et al. (2019).

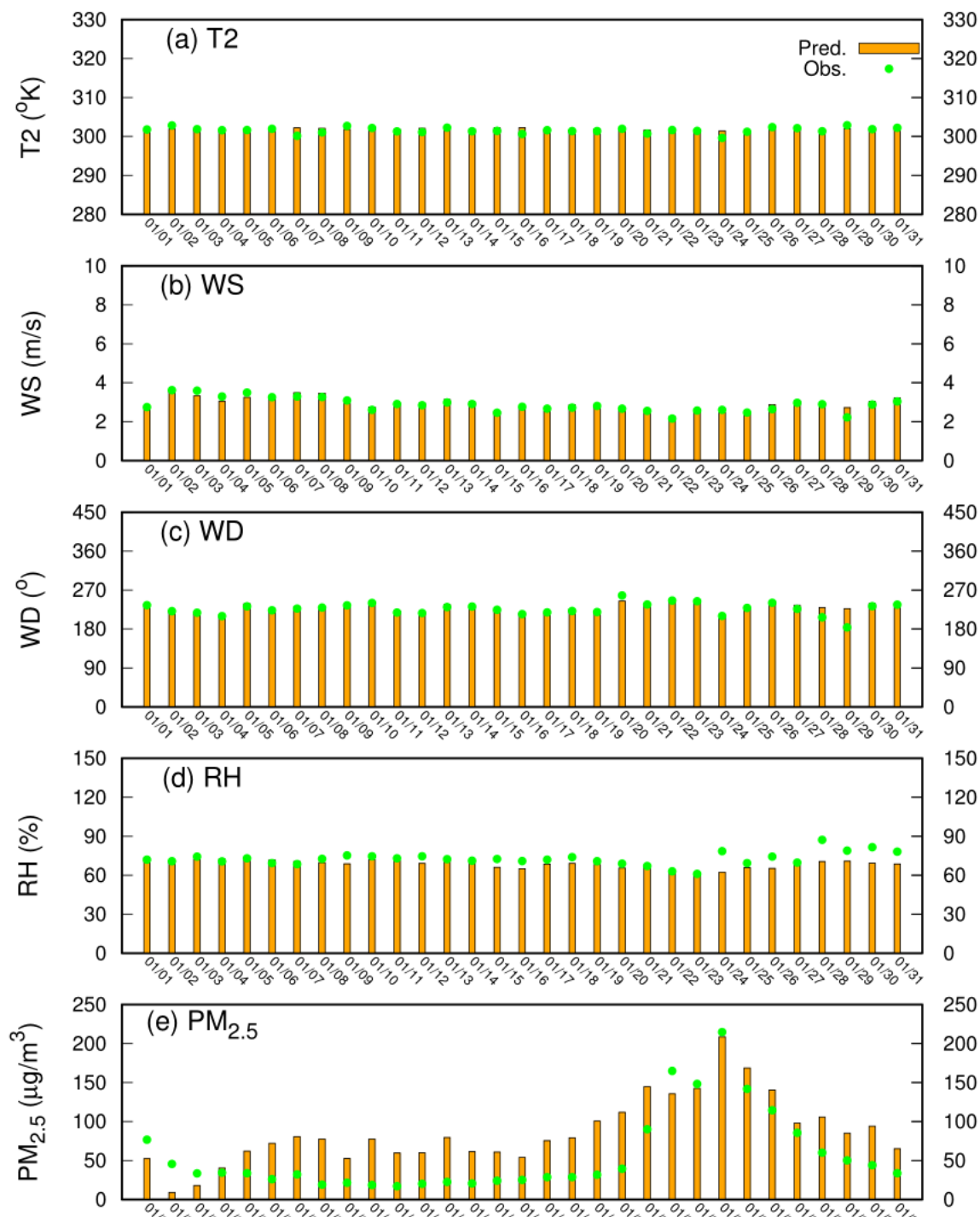
180

181 **3. Results and discussion**

182 *3.1. WRF model performance*

183 Previous studies have elucidated the crucial roles of meteorological factors in the
184 formation, transportation, as well as dissipation of fine particulate matter and other air
185 pollutants (Hua et al., 2021; Hu et al., 2016; Sulaymon, et al., 2021a, 2021d). Therefore,
186 in assuring the accuracy of air quality simulations, a robust and satisfactory WRF model
187 performance must be obtained. In evaluating the performance of WRF model, the
188 simulated temperature (T2) and relative humidity (RH) at 2 m above surface, and wind
189 speeds (WS) and wind directions (WD) at 10 m above ground level were compared with
190 observation data downloaded from the official website of the National Climate Data
191 Center (NCDC) (<ftp://ftp.ncdc.noaa.gov/pub/data/noaa/>, last accessed on October 30,
192 2022). The temporal variations of the meteorological variables and PM_{2.5} are illustrated
193 in Fig. 2. Table 1 provides the statistical indices, including the mean observation (OBS),
194 mean prediction (PRE), mean bias (MB), mean error (ME), and the root mean square

195 error (RMSE). With MB and ME values of 0.24 and 0.60, respectively, which fell below
 196 the suggested



197
 198 **Fig. 2.** Temporal variations of the predicted and observed meteorological variables
 199 (temperature, wind speed, wind direction, and relative humidity) and PM_{2.5}
 200 concentrations in Lagos during January 2021.

201

202 benchmarks ($MB \leq \pm 0.5$; $ME \leq 2.0$) (Emery et al., 2001), T2 (Fig. 2a) was well-reproduced
 203 by the WRF model. Similar statistical indices and model performance of T2 had been
 204 reported in the Beijing-Tianjin-Hebei (BTH) region of China during winter (January
 205 2014) (Lang et al., 2021). Wind speed was slightly over-estimated during the study
 206 period, however, considering the fact that its MB, ME, and RMSE indices were far below
 207 the suggested benchmarks (Table 1), the WRF model in this study showed a better
 208 performance in capturing the observed WS as illustrated in Fig. 2(b).

209 **Table 1.** Model performance of meteorological factors in Lagos, Nigeria (OBS: observed
 210 mean; PRE: predicted mean; MB: mean bias; ME: mean error; RMSE: root mean square
 211 error).

| | Metrics | January | Benchmarks |
|----------|---------|---------|----------------|
| T2 (K) | OBS | 301.6 | |
| | PRE | 301.8 | |
| | MB | 0.24 | $\leq \pm 0.5$ |
| | ME | 0.6 | ≤ 2.0 |
| | RMSE | 0.78 | |
| WS (m/s) | OBS | 2.87 | |
| | PRE | 2.90 | |
| | MB | 0.03 | $\leq \pm 0.5$ |
| | ME | 0.14 | ≤ 2.0 |
| | RMSE | 0.17 | ≤ 2.0 |
| WD (°) | OBS | 226.3 | |
| | PRE | 228.5 | |
| | MB | 2.17 | $\leq \pm 10$ |
| | ME | 5.69 | $\leq \pm 30$ |
| | RMSE | 9.90 | |
| RH (%) | OBS | 72.6 | |
| | PRE | 68.6 | |
| | MB | -4.04 | |
| | ME | 4.55 | |
| | RMSE | 6.21 | |

212

213 The over-estimation of WS might be due to unresolved topography in the WRF model (Li
214 et al., 2014). The statistical indices (MB and ME) of WS in this study are consistent with
215 those reported by Lang et al. (2021) and Sulaymon et al. (2021b). As illustrated in Fig.
216 2(c), the predominant WD during the study period was southwesterly. Similar to T2 and
217 WS, WD was also over-predicted during the simulation period. However, the predicted
218 WD showed better agreement with observations, having found both MB and ME indices
219 falling below the suggested benchmarks ($MB \leq \pm 10$; $ME \leq \pm 30$). Similar model
220 performance had been reported by Ma et al. (2021) and Qiao et al. (2019). Relative
221 humidity (Fig. 2d) was underpredicted with MB and ME values of -4.04 and 4.55,
222 respectively. Although, there are presently no performance benchmarks for RH. Previous
223 studies in India (Bhati and Mohan, 2018), China (Hu et al., 2016; Li et al., 2021;
224 Sulaymon et al., 2021a, 2021b), and Brazil (Kitagawa et al., 2021; Pedruzzi et al., 2021)
225 had also reported under-estimation of RH. Bhati and Mohan (2018) had linked under-
226 estimation of RH to the influence of boundary layer parameterization on meteorological
227 prediction. Generally, the WRF model performances in the present study were
228 satisfactory and better when compared to previous studies from other parts of the world
229 (Bhati and Mohan, 2018; Hu et al., 2016; Kitagawa et al., 2021; Kota et al., 2018;
230 Pedruzzi et al., 2021; Sulaymon et al., 2021a; Yu et al., 2021). Since the WRF model has
231 shown a robust and better performance in this study, the meteorological fields were
232 utilized in driving the air quality simulation.

233 3.2. *CMAQ model performance*

234 To evaluate the performance of the CMAQ model in reproducing the observed
235 $PM_{2.5}$ in Lagos, the model was evaluated based on some statistical indices, including the

236 mean observations (OBS), mean predictions (PRE), mean fractional bias (MFB), mean
 237 fractional error (MFE), mean normalized bias (MNB), and mean normalized error (MNE).
 238 The hourly PM_{2.5} observation data were downloaded from the official website of the
 239 United States of America (USA) Embassy, Lagos
 240 ([https://www.airnow.gov/international/us-embassies-and-consulates/#Nigeria\\$Lagos](https://www.airnow.gov/international/us-embassies-and-consulates/#Nigeria$Lagos), last
 241 accessed on October 30, 2022). Necessary quality checks were carried out on the data
 242 before being used for evaluation (Sulaymon et al., 2021c). The CMAQ model
 243 performances in predicting PM_{2.5} during January 2021 in Lagos are illustrated in Table 2.
 244 The observed PM_{2.5} concentration was well-simulated in Lagos, with the model
 245 performance indices falling within the recommended benchmarks (MFB $\leq \pm 0.60$; MFE \leq
 246 0.75) (Boylan and Russel, 2006). The temporal variations of the observed and simulated
 247 PM_{2.5} concentrations are illustrated in Fig. 2(e). With positive MFB (0.52), the CMAQ
 248 model over-predicted PM_{2.5} concentrations during the study period. Overall, the CMAQ
 249 model in this study has exhibited a good performance when compared to previous studies
 250 around the world (Jiang et al., 2021; Kitagawa et al., 2021; Kota et al., 2018; Mao et al.,
 251 2022; Pedruzzi et al., 2021; Sulaymon et al., 2021a; Tao et al., 2020). Therefore, the
 252 predicted PM_{2.5} concentrations were deemed acceptable for further analyses.

253 **Table 2.** Model performance of PM_{2.5} in Lagos, Nigeria (OBS: observed average; PRE:
 254 predicted average; MFB: mean fractional bias; MFE: mean fractional error; MNB: mean
 255 normalized bias; MNE: mean normalized error). The study period was January 2021. The
 256 performance benchmarks for PM_{2.5} were suggested by Boylan and Russell (2006).

| | Metrics | January | Benchmarks |
|--|---------|---------|-----------------|
| PM _{2.5} (µg/m ³) | OBS | 56.4 | |
| | PRE | 86.2 | |
| | MFB | 0.52 | $\leq \pm 0.60$ |
| | MFE | 0.69 | ≤ 0.75 |
| | MNB | 1.09 | |
| | MNE | 1.21 | |

257

258

259

260 3.3. *Statistical analysis of PM_{2.5} during different pollution levels*

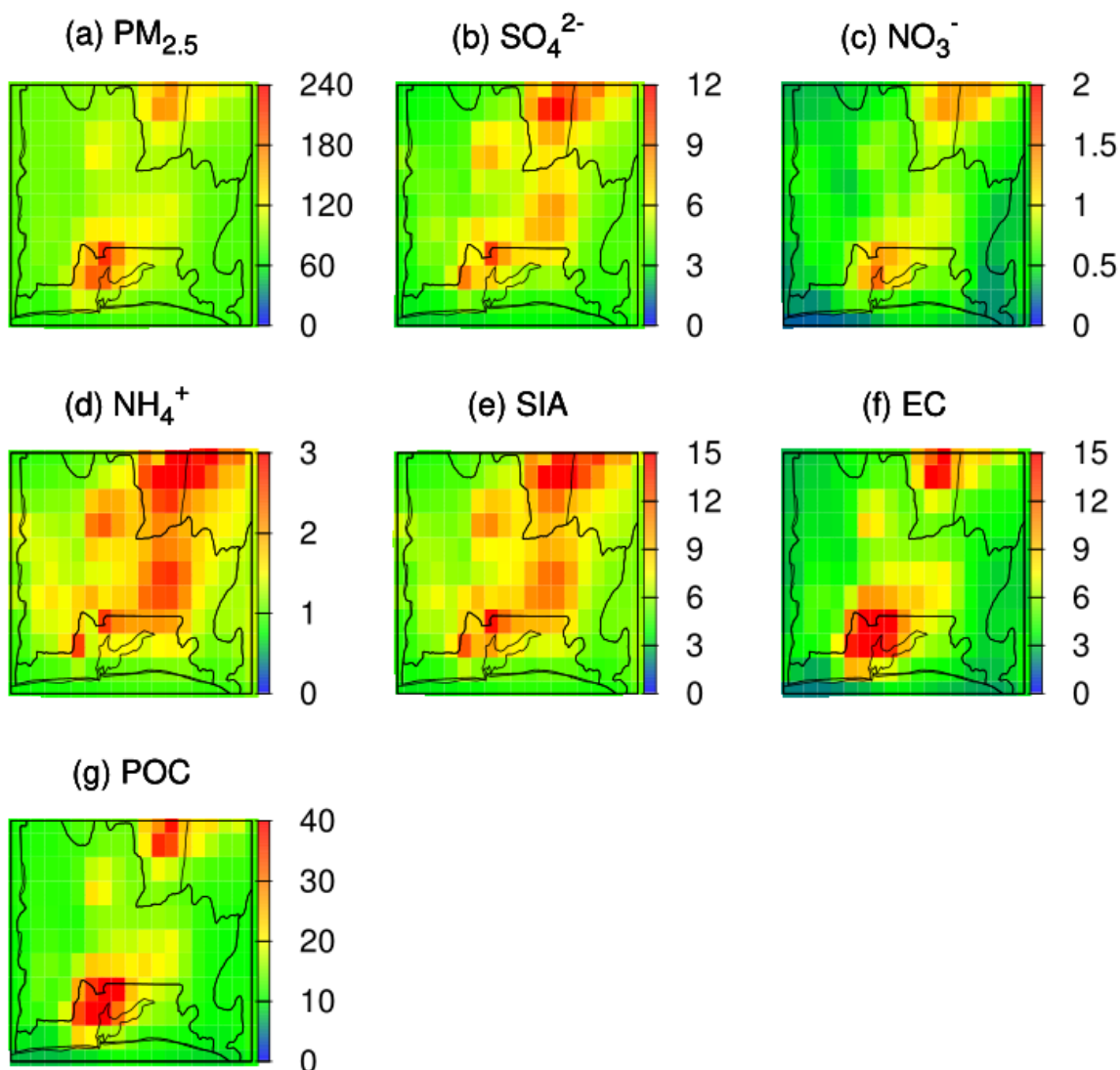
261 As illustrated in Fig. 2 (e), it can be observed that throughout the simulation
262 period (except on January 2 and 3), the 24-hr total PM_{2.5} concentrations in Lagos greatly
263 exceeded the old daily air quality guideline (AQG) level (25 µg/m³) recommended by the
264 World Health Organization (WHO, 2005). Furthermore, considering the new WHO AQG
265 level (15 µg/m³) (WHO, 2021) for PM_{2.5}, only one day (January 2 with PM_{2.5} value of
266 11.92 µg/m³) could be described as a clean day, while the remaining days witnessed
267 different levels of PM_{2.5} pollution, ranging from slight to severe pollution. Based on the
268 daily PM_{2.5} concentrations, air quality can be grouped into various pollution levels. In
269 this study, the PM_{2.5} pollution levels were categorized into five groups (Table S2). Table
270 S3 shows the statistical results of PM_{2.5} in January based on different pollution levels.
271 Under clean level, the simulated PM_{2.5} concentrations were below the old WHO AQG
272 level. However, the simulated maximum PM_{2.5} concentration exceeded the new AQG
273 value of WHO, indicating that even during the clean days, exposure to PM_{2.5} at low
274 levels could still cause adverse effects to human health. Under the slightly-polluted level,
275 there were 12 days with concentration range of $35 \leq \text{PM}_{2.5} < 75$. The simulated minimum,
276 maximum, and mean PM_{2.5} greatly breached the old and new AQG levels of WHO. For
277 instance, the simulated mean PM_{2.5} was 2.5 and 4.2 times the old and new AQG level,
278 respectively. Considering the moderately-polluted level (10 days with concentration

279 range of $75 \leq PM_{2.5} < 115$), it could be noted that the simulated mean $PM_{2.5}$ was 3.7 and
280 6.2 times the old and new AQG level, respectively. Under the heavily-polluted level, the
281 simulated mean $PM_{2.5}$ was 5.4 and 9.1 times the old and new AQG level, respectively.
282 The simulated $PM_{2.5}$ ranged between 167.3-198.6 $\mu\text{g}/\text{m}^3$, with mean of 182.9 $\mu\text{g}/\text{m}^3$.
283 $PM_{2.5}$ under the heavily-polluted level greatly exceeded the old and new AQG levels by
284 7.3 and 12.2 times, respectively. The results of this study showed that the residents of
285 Lagos were greatly exposed to high $PM_{2.5}$ pollution throughout January 2021, and this
286 could lead to adverse human health effects (Croft et al., 2019; Hopke et al., 2019; Shen et
287 al., 2020; Yan et al., 2018).

288 3.4. *Spatial variations of $PM_{2.5}$ and its major components during the pollution* 289 *episode*

290 The spatial distributions of the simulated $PM_{2.5}$ concentrations and its major
291 components during the study period are illustrated in Fig. 3. An atmospheric pollution
292 episode (APE) is said to occur when daily $PM_{2.5}$ concentration persistently exceeds 50
293 $\mu\text{g}/\text{m}^3$ (interim target 2 of WHO) (WHO, 2021) for at least two consecutive days
294 (Sulaymon et al., 2021b; Zhang et al., 2019). An APE occurred in January 2021, and was
295 characterized with high $PM_{2.5}$ concentrations. The APE ($50 \mu\text{g}/\text{m}^3 \leq PM_{2.5}$) lasted for 27
296 days (January 5-31). Spatially, highest $PM_{2.5}$ concentrations ($PM_{2.5} \geq 120 \mu\text{g}/\text{m}^3$) were
297 noted in the northwestern region of Lagos metropolis, while the rest of the city was
298 characterized with $60 \leq PM_{2.5} \leq 120 \mu\text{g}/\text{m}^3$. During the prolonged pollution episode, the
299 averaged city-wide concentration was 94.6 $\mu\text{g}/\text{m}^3$, while $PM_{2.5}$ concentrations in the
300 northwest were as high as 150-220 $\mu\text{g}/\text{m}^3$. This indicates the severity of $PM_{2.5}$ pollution
301 during the APE.

302 Among the three components that make the secondary inorganic aerosols (SIA),
303 sulfate (SO_4^{2-}) had the highest contributions, followed by ammonium (NH_4^+), and nitrate
304 (NO_3^-). Sulfate was evenly distributed across the city, with higher concentrations (6-15
305 $\mu\text{g}/\text{m}^3$) located in the northwestern and upper northern areas. For ammonium, higher
306 concentrations (2-3 $\mu\text{g}/\text{m}^3$) were found in the upper north and northwest areas, while
307 other areas were concentrated with 0.8-2 $\mu\text{g}/\text{m}^3$ of NH_4^+ . Similar to sulfate and
308 ammonium, nitrate also peaked in the northwest area. It can be deduced that among the
309 three SIA species, sulfate contributed most to $\text{PM}_{2.5}$.



310

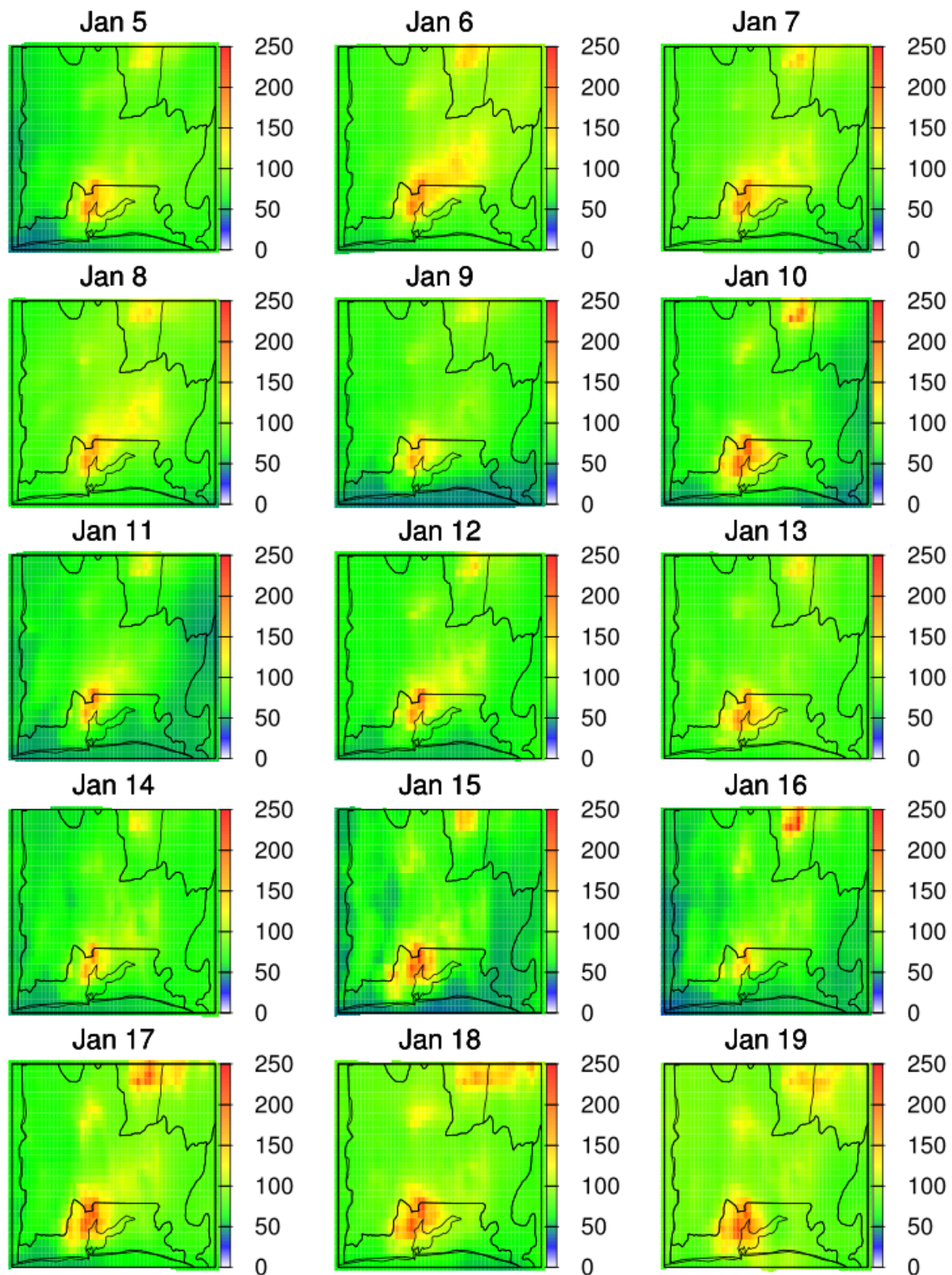
311 **Fig. 3.** Spatial distributions of the predicted total PM_{2.5} and its major components in
312 Lagos during the atmospheric pollution episode. Units are µg/m³.

313
314 Overall, SIA (sum of SO₄²⁻, NO₃⁻, and NH₄⁺) was evenly distributed over Lagos, with
315 higher concentrations (6-15 µg/m³) located in the northwestern, northern, and central
316 areas. In addition, during the pollution episode, the concentrations of elemental carbon
317 (EC) and primary organic carbon (POC) were notably very high in the northwestern area
318 of Lagos. The northwestern area (which includes Ikeja, Agege, Ifako-Ijaye, Oshodi,
319 Mushin, Shomolu, Surulere, and Ajegunle areas) is densely populated and highly
320 industrialized (Owoade et al., 2013), which results to high energy consumption. In
321 addition, the Muritala Muhammed International Airport (MMIA), which is the busiest
322 and largest international airport in Nigeria and West Africa, is located in the northwestern
323 part of Lagos. Generally, Lagos is characterized with heavy daily traffic (Okimiji et al.,
324 2021; Owoade et al., 2013), especially in the early morning and late afternoon (the local
325 rush hours). The northwestern region records more traffic than any other region. High
326 traffic volumes can be attributed to the presence of the administrative offices of several
327 governmental agencies as well as those of many private enterprises. Therefore, emissions
328 from local anthropogenic sources particularly in the northwestern region of the city are
329 likely the dominant contributors to the elevated PM_{2.5} concentrations. However, polluted
330 winds being transported from the neighboring cities in Ogun State, which borders Lagos
331 in the north could also aggravate the PM_{2.5} pollution, especially in the northwestern area
332 of Lagos.

333 3.5. *Spatiotemporal variations of PM_{2.5} during the pollution episode*

334 Fig. 4 shows the daily spatial variations of the predicted PM_{2.5} during the APE in
335 Lagos and its neighboring cities. Except in the northwestern area of Lagos, PM_{2.5}

336 concentrations in most parts of the city were less than $100 \mu\text{g}/\text{m}^3$ during the first 14 days
337 of the episode (January 5-18). This could be attributed to elevated PBLH during the
338 period (Fig. S1), since high PBLH values lead to reduced pollution level (Tao et al.,
339 2020). The higher PBLH were generally noted within Lagos metropolis and its
340 surroundings during January 5-18. Within Lagos, the PBLH ranged between 200 and 850
341 m, with an average regional value of 560 m. In the northwestern region, however, a very
342 intense pollution episode was observed throughout the period (January 5-18), with 100
343 $\mu\text{g}/\text{m}^3$ being the



344
 345
 346

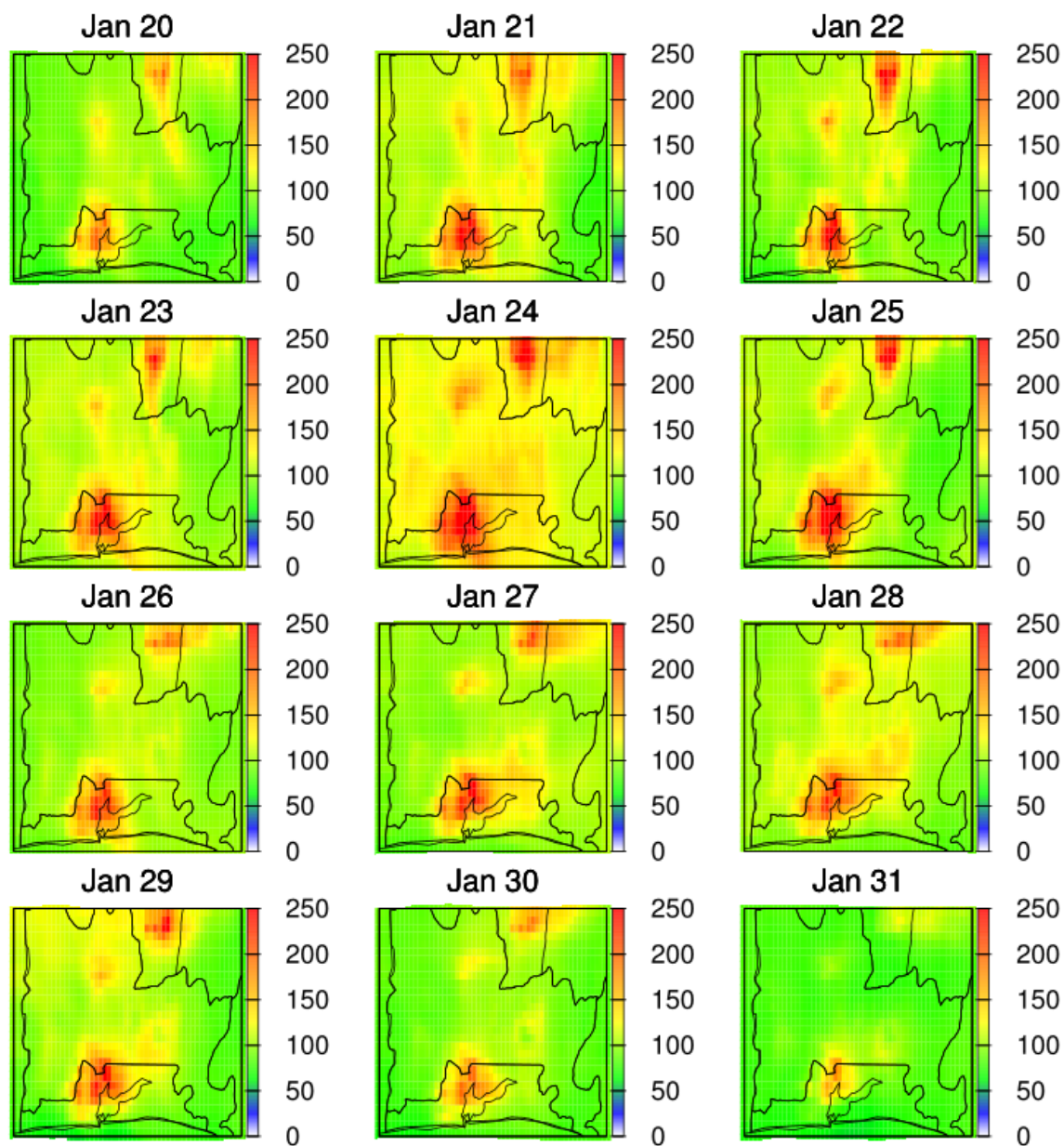
Fig. 4. Spatial distributions of the predicted total PM_{2.5} concentrations in Lagos during the atmospheric pollution episode. Units are µg/m³.

347 minimum regional daily PM_{2.5} concentration. As stated in section 3.4, the northwestern
348 region of Lagos is an urban area with several chemical industries and heavy traffic. Thus,
349 it is a major hub of anthropogenic emissions. During the first four days (January 5-8) of
350 the episode, high wind speeds (3-6 m/s) were observed in most of Lagos metropolis,
351 especially in the northwestern and central areas (Fig. S2). The APE began on January 5
352 (Fig. 4) with high haze ($50 \leq \text{PM}_{2.5} \leq 120 \mu\text{g}/\text{m}^3$) noted across the major parts of the
353 study area except at the northwestern area where a cluster of very high pollution ($150 \leq$
354 $\text{PM}_{2.5} < 200 \mu\text{g}/\text{m}^3$) was found. Prior to the inception of the city-wide heavy haze on
355 January 6, a high PM_{2.5} pollution cluster was initially noted in the northwestern area on
356 January 5 (Fig. 4). On January 6, a strong northwesterly wind (Fig. S2) enhanced the
357 transportation of pollutants to other parts of the Lagos metropolis. Due to the continuous
358 flow of the northwesterly winds, the PM_{2.5} pollution cluster that was initially formed in
359 the northwestern area on January 5, steadily got spread to and enveloped the entire study
360 area, with regional PM_{2.5} concentrations exceeding $100 \mu\text{g}/\text{m}^3$ on January 6 (Fig. 4). This
361 trend persisted until January 8. On several days (e.g January 9 and 11), the pollution was
362 low ($\text{PM}_{2.5} \leq 50 \mu\text{g}/\text{m}^3$) in most areas of Lagos (except the northern and central areas),
363 especially in the western and eastern parts of the city. With different pollution intensities
364 across Lagos and its surrounding cities, the APE continued till January 31. As previously
365 discussed and illustrated in Fig. 4, there were tendencies of cross-regional transport of
366 PM_{2.5} pollution from the surrounding cities (bordering Lagos to the north) into the study
367 area. The transported pollution could have aggravated the pollution level generally
368 caused by local anthropogenic emissions. Compared to January 16 (with moderate

369 pollution), higher pollution was noted across the Lagos metropolis on January 17 and 18,
370 with the highest being found in the northwestern area of the city.

371 Compared to the first 14 days, the PM_{2.5} concentrations across Lagos metropolis
372 and specifically in the northwestern area were relatively higher during the last 13 days of
373 the episode (January 19-31) (Fig. 4). During this period (January 19-31), the wind speed
374 in most of Lagos ranged between 2-4 m/s (Fig. S2), with the lowest values being
375 observed in the northwestern area. The lack of dispersion could have driven the severe
376 haze recorded in the northwestern region as lower wind speed reduces the dispersion of
377 pollutants (Sulaymon et al, 2021a). Generally, the PBLH within Lagos metropolis was
378 lower during January 19-30 compared to January 5-18. During January 19-30 of the APE,
379 the daily averaged PBLH was between 150-800 m, having an average regional value of
380 491 m. Generally, the formation of high PM_{2.5} pollution is enhanced by low PBLH and
381 WS (Li et al., 2019; Sulaymon et al, 2021a; Tao et al., 2020; Wang et al., 2020). For
382 instance, on January 19, a high PM_{2.5} concentration was noted in northwestern Lagos (Fig.
383 4). Due to the stagnant and low wind speeds (especially during January 19-25) across the
384 Lagos metropolis and specifically in the northwestern region, the APE persisted until
385 January 31. The pollution episode became more significant on January 21, with average
386 regional PM_{2.5} reaching 120 µg/m³, while the concentrations in the northwestern region
387 exceeded 200 µg/m³. The severe pollution continued until January 24 when it peaked
388 with the PM_{2.5} concentrations above 150 µg/m³ widely spread across the Lagos
389 metropolis and its surrounding cities in the north. The highest concentrations (PM_{2.5}>200
390 µg/m³) were not only found in the northwestern but also in the southwestern and southern
391 parts of Lagos nearest to the ocean. On January 25, severe haze was still recorded in the

392 northwestern and southern parts of Lagos, although lower than January 24. The other
393 areas had PM_{2.5}



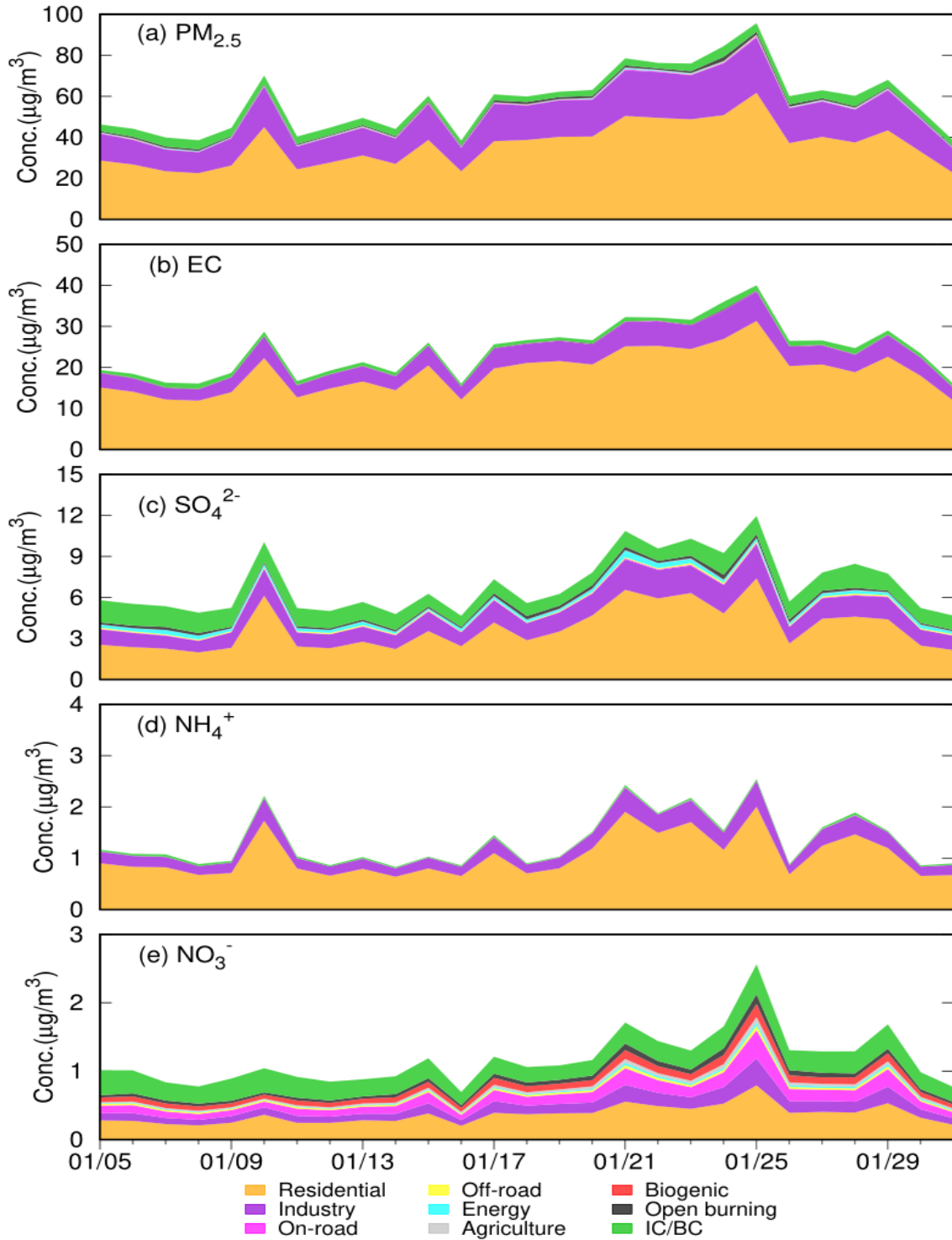
394
395 **Fig. 4.** (continued).

396 concentrations ranging between 60 and 120 µg/m³, and the haze persisted until January
397 31 when the APE ended with a decline to moderate to high regional pollution. With 27
398 days characterized with high PM_{2.5} concentrations during the episode, Lagos was

399 subjected to severe PM_{2.5} pollution during January 2021. Therefore, quantifying the
400 contributions from each emission sector to total PM_{2.5} and its major components during
401 the APE became highly imperative, as the results would provide scientific basis for
402 designing and implementing effective emission control strategies towards abating PM_{2.5}
403 pollution in the city.

404 3.6. *Source apportionment of PM_{2.5} and its major components*

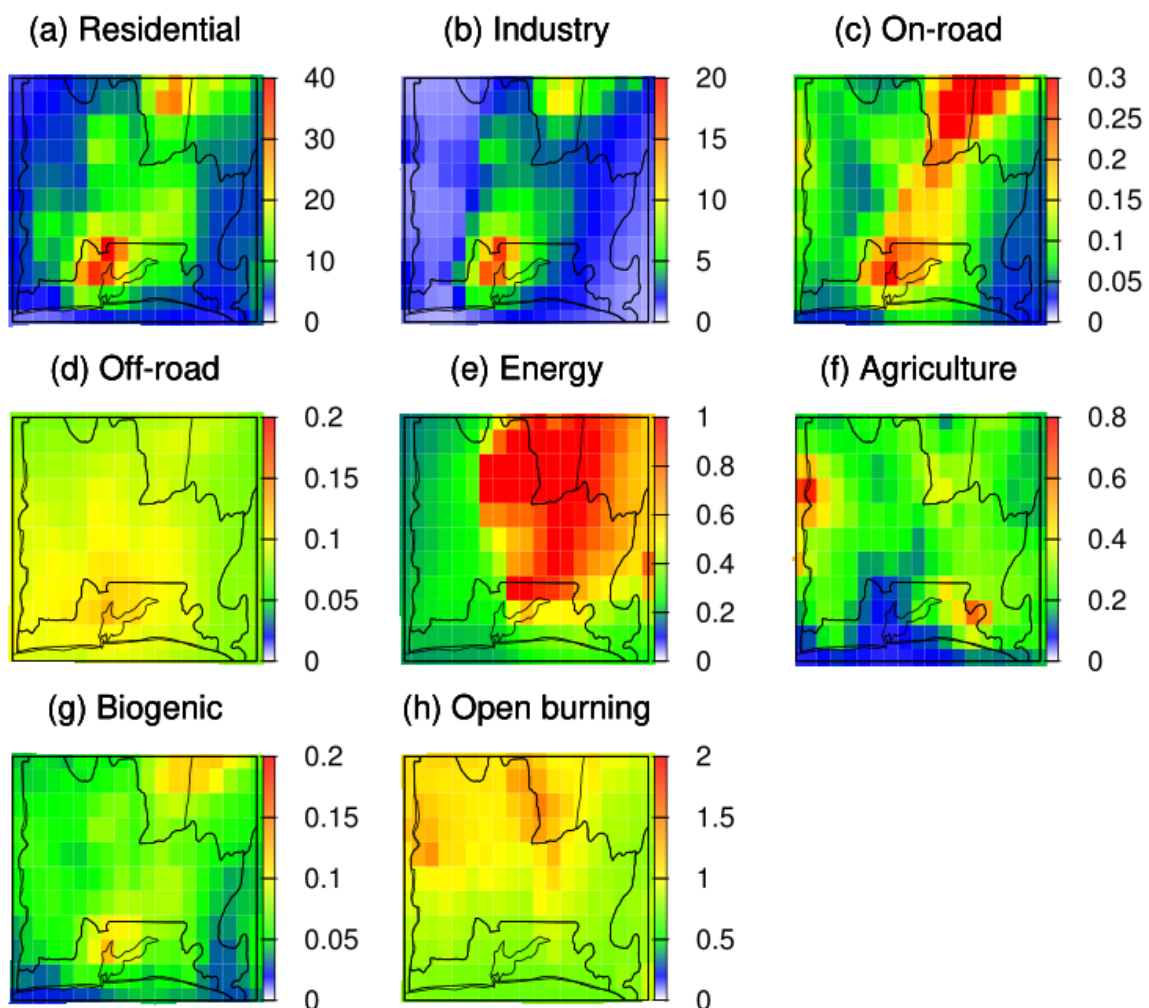
405 The temporal variations of the contributions of different sources to daily PM_{2.5}
406 and its major components in Lagos during the APE are illustrated in Fig. 5. During the
407 study period, the averaged contributions of residential, industry, open burning, and IC/BC
408 to total PM_{2.5} (Fig. 5a) in Lagos were 36.2, 16.5, 0.78, and 3.57 µg/m³, respectively. The
409 three major sources of EC (Fig. 5b) were residential, industry, and ICBC, with averaged
410 contributions of 18.9, 4.46, and 1.00 µg/m³, respectively. Following the same
411 arrangement of the sources for EC, the contributions of the sectors towards SO₄²⁻ (Fig. 5c)
412 were 3.71, 1.43, and 1.25 µg/m³, respectively. In addition to the three major sources of
413 SO₄²⁻, there were also slight contributions from energy and open burning sectors on most
414 of the days of the episode. For NH₄⁺ (Fig. 5d), residential and industry were the dominant
415 sectors with averaged contributions of 1.04 and 0.27 µg/m³, respectively. The
416 contributions from on-road transport, off-road transport, energy, agriculture, and biogenic
417 sectors to PM_{2.5}, EC, and NH₄⁺ were very low. Considering NO₃⁻ (Fig. 5e), all of the
418 emission sectors contributed towards its daily formation, with residential, industry, and
419 on-road serving as the three major contributors. It should be noted that the contributions
420 of residential and industry sectors were generally higher during the last 13 days of the
421 episode than the first 14 days of the episode.



422
 423
 424
 425

Fig. 5. Daily contributions of emissions sectors to the predicted (a) total $\text{PM}_{2.5}$, (b) EC, (c) SO_4^{2-} , (d) NH_4^+ , and (e) NO_3^- during the atmospheric pollution episode.

426 Fig. 6 illustrates the spatial distributions of various source contributions to the
 427 averaged total $PM_{2.5}$ in Lagos during the episode. High contributions from residential
 428 ($20\text{-}40\ \mu\text{g}/\text{m}^3$) and industry ($10\text{-}20\ \mu\text{g}/\text{m}^3$) were found in the northwestern area of the city.
 429 In other areas of Lagos, the contributions of residential and industrial emissions were up
 430 to $20\ \mu\text{g}/\text{m}^3$ and $10\ \mu\text{g}/\text{m}^3$, respectively. This is consistent with the results of Guo et al.
 431 (2017).



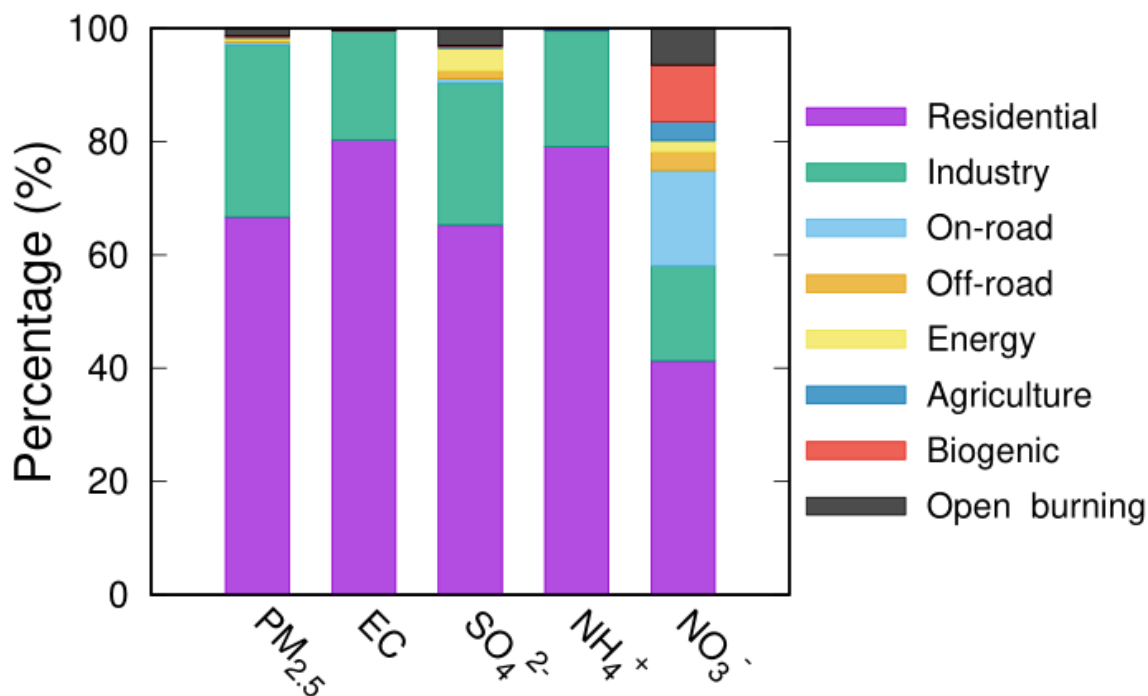
432 **Fig. 6.** Source apportionment of total $PM_{2.5}$ from (a) residential, (b) industry, (c) on-road,
 433 (d) off-road, (e) energy, (f) agriculture, (g) biogenic, and (h) open burning during the
 434 atmospheric pollution episode. Units are $\mu\text{g}/\text{m}^3$.
 435

436

437 Guo et al. (2017) had previously used EDGAR emissions inventory in a source-oriented
438 CMAQ model for the source apportionment of PM_{2.5} in North India, and found
439 residential emissions as the highest contributor, followed by industrial sector. In addition,
440 the elevated PM_{2.5} concentrations in major Chinese cities during winter period had been
441 linked to residential burning for heating purposes, industrial emissions, construction
442 activities, and road dust (Guo et al., 2020). PM_{2.5} contributed by open burning was up to
443 1 µg/m³, and uniformly distributed across the city. Energy also contributed up to 1 µg/m³,
444 especially in the upper northern areas. The contributions from other emissions sectors to
445 PM_{2.5} during the pollution episode were low (less than 1 µg/m³) across the city.

446 The percentage contributions of emission sectors to PM_{2.5} and its major
447 components during the APE are shown in Fig. 7, with residential and industrial sectors
448 dominating. The contributions of residential to PM_{2.5}, EC, SO₄²⁻, and NH₄⁺ were 66.7,
449 80.3, 65.3, and 79.1%, respectively, while the industry contributed 30.4, 19.0, 25.1, and
450 20.4% to PM_{2.5}, EC, SO₄²⁻, and NH₄⁺, respectively. Energy and open burning also
451 notably contributed to SO₄²⁻, with 4.0 and 3.1%, respectively. For NO₃⁻, the contributions
452 of residential, industry, on-road, biogenic, open burning, agriculture, off-road, and energy
453 were 41.3, 16.8, 16.8, 10.0, 6.5, 3.4, 3.3, and 2.0%, respectively. These findings are
454 consistent with the results of Zhao et al. (2021), where industrial and residential sectors
455 were the major contributors to PM_{2.5} in six cities of East-central China during the
456 COVID-19 lockdown. The dominance of residential sector could be attributed to the
457 cooking activities by the dense population of Lagos residents, while the dominance of
458 industrial sector could be associated with emissions from large-scale industries in the city.
459 Also, Li et al. (2020) and Ma et al. (2021) had reported residential and industrial sectors

460 as the dominant contributors to PM_{2.5} in YRD region, China. Furthermore, residential and
 461 industry were the major emission sectors contributing to PM_{2.5} in the BTH region of
 462 China, especially during winter season (Chang et al., 2019).



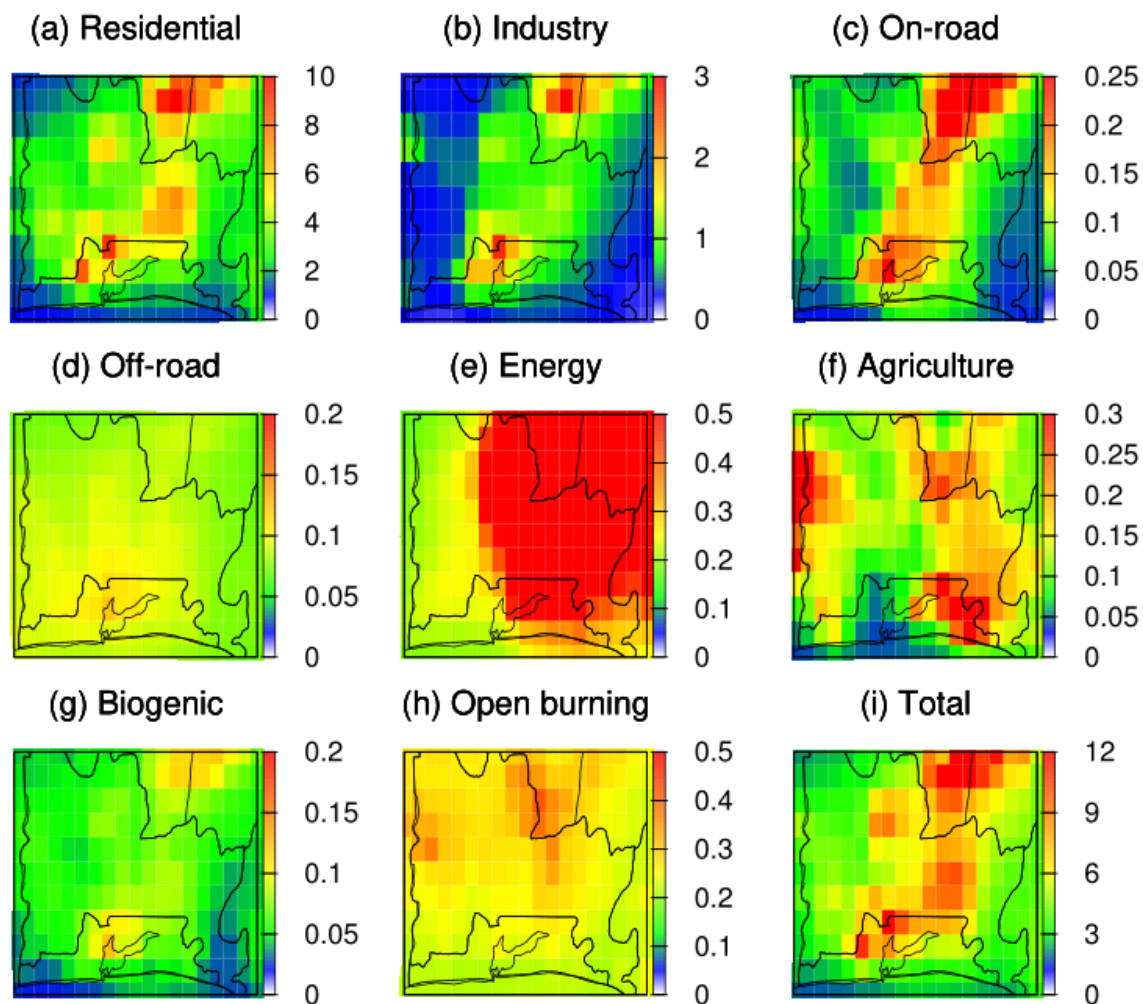
463
 464 **Fig. 7.** Contributions of different emissions sectors to total PM_{2.5} and its major
 465 components during the atmospheric pollution episode.

466

467 3.7. Source apportionment of secondary inorganic aerosols (SIA)

468 Previous studies have identified the secondary inorganic aerosols (sulfate, nitrate,
 469 and ammonium) as the major components of total PM_{2.5} (Guo et al., 2017; Li et al., 2021;
 470 Shi et al., 2017). The contributions of different emissions sectors to SIA are shown in Fig.
 471 8, while the source contributions to SO₄²⁻, NO₃⁻, and NH₄⁺ are illustrated in Figs S3, S4,
 472 and S5, respectively. Similar to PM_{2.5}, residential and industry served as the major
 473 emission sectors contributing to SIA. Considering the total contributions of all the
 474 emissions sectors to SIA during the APE (Fig. 8i), higher concentrations of SIA were

475 majorly concentrated in the northwest, upper north, and central areas of Lagos, and were
 476 dominated by the contributions from residential ($\sim 9 \mu\text{g}/\text{m}^3$) and industry ($\sim 3 \mu\text{g}/\text{m}^3$) as
 477 illustrated in Figs 8(a) and 8(b), respectively, while other areas were filled with low but
 478 substantive SIA concentrations ($3\text{-}6 \mu\text{g}/\text{m}^3$) (Fig. 8i).



479 **Fig. 8.** Source apportionment of SIA from (a) residential, (b) industry, (c) on-road, (d)
 480 off-road, (e) energy, (f) agriculture, (g) biogenic, and (h) open burning during the
 481 atmospheric pollution episode. Units are $\mu\text{g}/\text{m}^3$.
 482

483
 484 High contributions from residential ($2\text{-}9 \mu\text{g}/\text{m}^3$) were located in the north and central
 485 areas of Lagos, while up to $3 \mu\text{g}/\text{m}^3$ contributions due to industry were located in the
 486 northwest. The contributions from other emission sectors to SIA were very low. As

487 shown in Fig. S3, residential and industry were the dominant sources of sulfate. Sulfate
488 concentrations from residential (up to $6 \mu\text{g}/\text{m}^3$) and industry ($\sim 2 \mu\text{g}/\text{m}^3$) are concentrated
489 in the north of Lagos (particularly the northwest), as the region is densely populated and
490 highly industrialized. Residential, industry, and on-road transport sectors were the major
491 sources of nitrate (Fig. S4). Furthermore, only residential and industry served as the
492 major sectors contributing to NH_4^+ (Fig. S5). Just as the concentrations of $\text{PM}_{2.5}$ were
493 higher during the APE, higher SIA concentrations were also noted during the study
494 period. This reveals the severity of $\text{PM}_{2.5}$ pollution in Lagos during the pollution episode
495 in January 2021. Overall, the substantive contributions of residential and industry sectors
496 to $\text{PM}_{2.5}$ and SIA during the APE suggests that controlling residential and industrial
497 emissions would pave way towards reducing $\text{PM}_{2.5}$ and its major components in Lagos.

498 3.8. *Influence of meteorological factors on $\text{PM}_{2.5}$ pollution*

499 Previous studies have revealed that meteorological factors such as high RH, low
500 WS, and low PBLH hinder the dispersion of atmospheric pollutants, resulting into the
501 formation of severe air pollution, especially during the cold season (Li et al., 2019; Liu et
502 al., 2016; Sulaymon et al., 2021a; Wang et al., 2020; Zhang et al., 2019). As earlier
503 discussed, low PBLH (Fig. S1) and WS (Fig. S2) were noted across Lagos during the
504 study period. Therefore, the ventilation coefficient (VC) was used to evaluate the
505 effectiveness of atmospheric dispersion during the APE period. VC (in m^2s^{-1}) was
506 obtained as the product of WS and PBLH. Previous studies have widely employed VC in
507 evaluating the efficiency of atmospheric dispersion of air pollutants (Dai et al., 2020;
508 Sulaymon et al., 2021a; Tiwari et al., 2019), hence, further details about VC can be found
509 in the referenced studies. The temporal variations of $\text{PM}_{2.5}$ and VC in Lagos during

510 January are illustrated in Fig. S6. As a result of poor dispersion, low VC values (<2000
511 m²/s) were generally noted during the APE period, an indication of very high PM_{2.5}
512 pollution. During January 2-3 and 6-9, however, highest VC values were observed,
513 indicating that the PM_{2.5} pollution during those days was low compared to the last 15
514 days of the month (especially January 17-30). Low VC enhanced the accumulation of
515 high PM_{2.5} concentrations (Dai et al., 2020; Tiwari et al., 2019), which subsequently led
516 to the prolonged high-pollution days during the study period, especially during January
517 17-30. For instance, the VC on January 2 (1844.1 m²s⁻¹) was the highest, and it was
518 approximately twice the VC on January 24 (1017.9 m²s⁻¹), when the APE attained its
519 peak. Correspondingly, the highest PM_{2.5} concentration (208.7 µg/m³) occurred on
520 January 24, the same day with the lowest VC.

521 Furthermore, the influence of meteorological factors on PM_{2.5} was assessed using
522 the Pearson correlation analysis between PM_{2.5} concentrations and four meteorological
523 parameters (WS, PBLH, RH, and T2) during the APE. PM_{2.5} was negatively correlated
524 with WS ($r^2=-0.535$) and PBLH ($r^2=-0.539$). Zhang et al. (2019) had reported negative
525 correlations between PM_{2.5} and WS and PBLH. Sulaymon et al. (2021c, 2021d) and
526 Zhang et al. (2015) also reported an inverse relationship between PM_{2.5} and WS. In
527 addition, the association between PM_{2.5} and RH was negative ($r^2=-0.456$). The negative
528 correlation found between RH and PM_{2.5} in this study is consistent with those previously
529 reported in Lagos (Okimiji et al., 2021), Wuhan (Sulaymon et al., 2021c), Dhaka (Islam
530 et al., 2015), and Kathmandu (Giri et al., 2008). Negative correlations were also found
531 between PM_{2.5} and RH in Shanghai and Guangzhou (Zhang et al., 2015), especially
532 during the winter period. Considering the relationship between PM_{2.5} and temperature,

533 PM_{2.5} also exhibited negative correlation with T2 ($r^2=-0.347$) during the APE, which is
534 contrary to the findings of Okimiji et al. (2021) and Zhang et al. (2015) during winter.
535 However, the inverse correlation found between T2 and PM_{2.5} in this study is consistent
536 with previous studies in Kathmandu (Giri et al., 2008) and Hefei and Suzhou (Sulaymon
537 et al., 2021d), and was attributed to the cooling effect of particulate matter as a result of
538 its negative radioactive forces (Islam et al., 2015). The results of this study also showed
539 that the elevated PM_{2.5} concentrations in Lagos during the APE were aggravated by
540 unfavorable meteorological conditions. Therefore, when designing emission control
541 strategies towards reducing the level of PM_{2.5} in Lagos, it is very important to understand
542 the crucial roles being played by both chemistry and meteorology in the formation,
543 transportation, and dispersion of air pollutants as revealed in this study.

544 **4. Conclusions**

545 This study investigated the source apportionment of PM_{2.5} and its major
546 components in Lagos during a prolonged severe atmospheric pollution episode in January
547 2021, using the CMAQ-ISAM model. The influence of meteorological factors on PM_{2.5}
548 concentrations during the atmospheric pollution episode was also elucidated. The WRF
549 model reasonably and well-simulated the meteorological fields (temperature, wind speed,
550 wind direction, and relative humidity) for the CMAQ model, while the CMAQ model
551 exhibited good performances in reproducing the observed PM_{2.5} concentration during the
552 simulation period. Spatially, elevated PM_{2.5} concentrations were found in the
553 northwestern region of Lagos, an urban area with larger anthropogenic emissions. The
554 formation of elevated PM_{2.5} during the APE was greatly enhanced by low WS and PBLH.
555 The results of the ISAM showed that residential and industry sectors were the major

556 contributors to PM_{2.5} and SIA concentrations in Lagos during the APE. Residential and
557 industry contributed about 40 µg/m³ and 20 µg/m³, respectively to total PM_{2.5}. SO₄²⁻
558 accounted for the largest fraction of PM_{2.5}, attaining 6.0 µg/m³, with residential, industry,
559 and energy being its major sources. Residential, industry, and on-road sectors dominated
560 the contributions to NO₃⁻, while residential and industry served as the major sources of
561 NH₄⁺. Also, this study improves the understanding of the mechanisms that resulted to the
562 prolonged atmospheric pollution episode in Lagos under diverse meteorological
563 influences. The results of this study reveal that the control of PM_{2.5} pollution in Lagos is
564 urgently required, and this could be achieved by substantially reducing the emissions
565 from residential and industry sectors in Lagos and its neighboring cities.

566 **Acknowledgements**

567 This work was supported by the National Natural Science Foundation of China
568 (42007187).

569

570 **Conflict of Interest**

571 The authors declare that they have no conflict of interest.

572

573 **Open Research**

574 The code for the CMAQ model could be obtained from the website of the United States
575 Environmental Protection Agency (<https://www.epa.gov/cmaq/access-cmaq-source-code>,
576 last access: October, 2022) and the code of WRF model is available on the WRF users'
577 page (https://www2.mmm.ucar.edu/wrf/users/download/get_sources.html, last access:
578 October, 2022). The Emissions Database for Global Atmospheric Research (EDGAR)

579 can be found online (https://edgar.jrc.ec.europa.eu/dataset_ap50, last access: October,
580 2022). The Fire INventory from NCAR (FINN) can be download
581 (<https://www.acom.ucar.edu/Data/fire/>, last access: October 2022). The meteorological
582 observation is publicly available on the official website of the National Climate Data
583 Center (NCDC) (<ftp://ftp.ncdc.noaa.gov/pub/data/noaa/>, last access: October 2022). The
584 hourly PM_{2.5} observation data can be downloaded online
585 ([https://www.airnow.gov/international/us-embassies-and-consulates/#Nigeria\\$Lagos](https://www.airnow.gov/international/us-embassies-and-consulates/#Nigeria$Lagos), last
586 access: October 2022). The simulated data (PM_{2.5}, its major components, and
587 meteorological factors) and the observation data (PM_{2.5} and meteorological factors) used
588 for postprocessing (Figures and tables) in this study can be accessed online
589 (<https://doi.org/10.5281/zenodo.7409425>). All of the figures were created by the Python
590 Programming Language version 3.8 (<https://www.python.org/downloads/>, last access:
591 October 2022).

592

593 **References**

- 594 Abiye, O.E., Obioh, I.B., and Ezech, G.C.: Elemental characterization of urban
595 particulates at receptor locations in Abuja, north-Central Nigeria. *Atmos. Environ.*
596 81, 695-701, 2013.
- 597 Abiye, O.E., Obioh, I.B., Ezech, G.C., Alfa, A., Ojo, E.O., and Ganiyu, A.K.: Receptor
598 modeling of atmospheric aerosols in Federal Capital Territory (FCT), Nigeria.
599 *IFE J.Sci.* 16, 107-119, 2014.
- 600 Albuquerque, T.T. de A., Andrade, M.D.F., Ynoue, R.Y., Moreira, D.M., Andre~ao, W.L.,
601 and Soares, F.: WRF-SMOKE-CMAQ Modeling System for Air Quality
602 Evaluation in S~ao Paulo Megacity with a 2008 Experimental Campaign Data,
603 <https://doi.org/10.1007/s11356-018-3583-9>, 2018.
- 604 Albuquerque, T.T. de A., West, J., Andrade, M. de F., Ynoue, R., Andre~ao, W.L., Santos,
605 F. S. dos, Maciel, F.M., Pedruzzi, R., Mateus, V. de O., Martins, J.A., Martins,
606 L.D., Nascimento, E.G.S., and Moreira, D.M.: Analysis of PM_{2.5} concentrations under
607 pollutant emission control strategies in the metropolitan area of S~ao Paulo,
608 Brazil. *Environ. Sci. Pollut. Res.* 26, 33216-33227,
609 <https://doi.org/10.1007/s11356-019-06447-6>, 2019.

610 Andreão, W.L., Pinto, J.A., Pedruzzi, R., Kumar, P., and Albuquerque, T.T.de A.:
611 Quantifying the impact of particle matter on mortality and hospitalizations in four
612 Brazilian metropolitan areas. *J. Environ. Manage.* 270,
613 <https://doi.org/10.1016/j.jenvman.2020.110840>, 2020.

614 Appel, K.W., Bash, J., Fahey, K., Foley, K., Gilliam, R., Hogrefe, C., Hutzell, W., Kang,
615 D., Mathur, R., Murphy, B., Napelenok, S., Nolte, C., Pleim, J., Pouliot, G., Pye,
616 H., Ran, L., Roselle, S., Sarwar, G., Schwede, D., Sidi, F., Spero, T., and Wong,
617 D.: The community multiscale air quality (CMAQ) model versions 5.3 and 5.3.1:
618 system updates and evaluation. *Geosci. Model Dev. Discuss.* 1-41,
619 <https://doi.org/10.5194/gmd-2020-345>, 2020.

620 Bhati, S. and Mohan, M.: WRF-urban canopy model evaluation for the assessment of
621 heat island and thermal comfort over an urban airshed in India under varying land
622 use/land cover conditions. *Geoscience Letters*, 5(1),
623 <https://doi.org/10.1186/s40562-018-0126-7>, 2018.

624 Boylan, J. W. and Russel, A. G.: PM and light extinction model performance metrics,
625 goals, and criteria for three-dimensional air quality models. *Atmos.*
626 *Environ.*, 40, 4946-4959, <https://doi.org/10.1016/j.atmosenv.2005.09.087>, 2006.

627 Chang, X., Wang, S., Zhao, B., Xing, J., Liu, X., Wei, L., Song, Y., Wu, W., Cai, S.,
628 Zheng, H., Ding, D., and Zheng, M.: Contributions of inter-city and regional
629 transport to PM_{2.5} concentrations in the Beijing-Tianjin-Hebei region and its
630 implications on regional joint air pollution control. *Science of the Total*
631 *Environment*, 660, 1191- 1200, <https://doi.org/10.1016/j.scitotenv.2018.12.474>, 2019.

632 Crippa, M., Solazzo, E., Huang, G., Guizzardi, D., Koffi, E., Muntean, M., Schieberle, C.,
633 Friedrich, R., and Janssens-Maenhout, G.: High resolution temporal profiles in
634 the Emissions Database for Global Atmospheric Research. *Scientific Data*, 7(1),
635 <https://doi.org/10.1038/s41597-020-0462-2>, 2020.

636 Croft, D. P., Zhang, W., Lin, S., Thurston, S. W., Hopke, P. K., Masiol, M., Squizzato, S.,
637 van Wijngaarden, E., Utell, M. J., and Rich, D. Q.: The association between
638 respiratory infection and air pollution in the setting of air quality policy and
639 economic change. *Annals of the American Thoracic Society*, 16(3), 321–330,
640 <https://doi.org/10.1513/AnnalsATS.201810-691OC>, 2019

641 Dai, Q., Liu, B., Bi, X., Wu, J., Liang, D., Zhang, Y., Feng, Y., and Hopke, P. K.:
642 Dispersion normalized PMF provides insights into the significant changes in
643 source contributions to PM_{2.5} after the CoviD-19 outbreak. *Environmental Science and*
644 *Technology*, 54(16), 9917-9927, <https://doi.org/10.1021/acs.est.0c02776>, 2020.

645 Emery, C., Liu, Z., Russell, A.G., Odman, M.T., Yarwood, G., and Kumar, N.:
646 Recommendations on statistics and benchmarks to assess photochemical model
647 performance. *J. Air Waste Manag. Assoc.* 67 (5), 582-598,
648 <https://doi.org/10.1080/10962247.2016.1265027>, 2017.

649 Giri, D., Murthy, K.V., and Adhikary, P.R.: The Influence of Meteorological Conditions
650 on PM10 Concentrations in Kathmandu Valley. *Int. J. Environ. Res.*, 2, 49-60,
651 2008

652 Global Burden of Disease (GBD): Global age-sex-specific fertility, mortality,
653 healthy life expectancy (HALE), and population estimates in 204 countries and
654 territories, 1950-2019: a comprehensive demographic analysis for the Global
655 Burden of Disease Study 2019, *Lancet* 396: 1135-1159, 2020.

656 Gong, K., Li, L., Li, J., Qin, M., Wang, X., Ying, Q., Liao, H., Guo, S., Hu, M., Zhang,
657 Y., and Hu, J.: Quantifying the Impacts of Inter-City Transport on Air Quality in the
658 Yangtze River Delta Urban Agglomeration, China: Implications for Regional
659 Cooperative Controls of PM_{2.5} and O₃. *Sci. Total Environ.*, 779, 146619, 2021.

660 Guenther, A. B., Jiang, X., Heald, C. L., Sakulyanontvittaya, T., Duhl, T., Emmons, L. K.,
661 and Wang, X.: The Model of Emissions of Gases and Aerosols from Nature
662 version 2.1 (MEGAN2.1): An extended and updated framework for modeling
663 biogenic emissions. *Geosci. Model Dev.*, 5, 1471-1492,
664 <https://doi.org/10.5194/gmdd-5-1-2012>, 2012.

665 Guo, D., Wang, R., and Zhao, P.: Spatial distribution and source contributions of PM_{2.5}
666 concentrations in Jincheng, China. *Atmos. Pollut. Res.*, 11(8), 1281-1289,
667 [10.1016/j.apr.2020.05.004](https://doi.org/10.1016/j.apr.2020.05.004), 2020.

668 Guo, H., Kota, S. H., Sahu, S. K., Hu, J., Ying, Q., Gao, A., and Zhang, H.: Source
669 apportionment of PM_{2.5} in North India using source-oriented air quality models.
670 *Environmental Pollution*, 231, 426-436,
671 <https://doi.org/10.1016/j.envpol.2017.08.016>, 2017.

672 Guo, H., Han, F., Wang, Z., Pardue, J., and Zhang, H.: Deposition of sulfur and nitrogen
673 components in Louisiana in August, 2011. *Sci. Tot. Environ.*, 636, 124-133,
674 <https://doi.org/10.1016/j.scitotenv.2018.04.258>, 2018.

675 Guo, H., Kota, S. H., Sahu, S. K., and Zhang, H.: Contributions of local and regional
676 sources to PM_{2.5} and its health effects in north India. *Atmos. Environ.*, 214,
677 <https://doi.org/10.1016/j.atmosenv.2019.116867>, 2019.

678 Guttikunda, S.K. and Jawahar, P.: Atmospheric emissions and pollution from the
679 coalfired thermal power plants in India. *Atmos. Environ.* 92, 449-460, 2014.

680 Hopke, P. K., Croft, D., Zhang, W., Lin, S., Masiol, M., Squizzato, S., Thurston, S. W.,
681 van Wijngaarden, E., Utell, M. J., and Rich, D. Q.: Changes in the acute response
682 of respiratory diseases to PM_{2.5} in New York State from 2005 to 2016. *Science of
683 the Total Environment*, 677, 328-339,
684 <https://doi.org/10.1016/j.scitotenv.2019.04.357>, 2019.

685 Hua, J., Zhang, Y., de Foy, B., Shang, J., Schauer, J. J., Mei, X., Sulaymon, I. D., and
686 Han, T.: Quantitative estimation of meteorological impacts and the COVID-19
687 lockdown reductions on NO₂ and PM_{2.5} over the Beijing area using Generalized
688 Additive Models (GAM). *Journal of Environmental Management*, 291,
689 <https://doi.org/10.1016/j.jenvman.2021.112676>, 2021.

690 Hu, J., Zhang, H., Ying, Q., Chen, S.H., Vandenberghe, F., and Kleeman, M.J.: Long-
691 term particulate matter modeling for health effect studies in California – Part I:
692 Model performance on temporal and spatial variations. *Atmospheric Chemistry
693 and Physics*, 15, 3445-3461, <https://doi.org/10.5194/acp-15-3445-2015>, 2015a.

694 Hu, J., Wu, L., Zheng, B., Zhang, Q., He, K., Chang, Q., Li, X., Yang, F., Ying, Q., and
695 Zhang, H.: Source contributions and regional transport of primary particulate
696 matter in China. *Environmental Pollution*, 207, 31-42.
697 <https://doi.org/10.1016/j.envpol.2015.08.037>, 2015b.

698 Hu, J., Chen, J., Ying, Q., and Zhang, H.: One-year simulation of ozone and particulate
699 matter in China using WRF/CMAQ modeling system. *Atmospheric Chemistry
700 and Physics*, 16(16), 10333-10350, <https://doi.org/10.5194/acp-16-10333-2016>, 2016.

701 Hu, J., Li, X., Huang, L., Ying, Q., Zhang, Q., Zhao, B., Wang, S., and Zhang, H.:
702 Ensemble prediction of air quality using the WRF/CMAQ model system for
703 health effect studies in China. *Atmospheric Chemistry and Physics*, 17, 13103-13118,
704 <https://doi.org/10.5194/acp-17-13103-2017>, 2017.

705 Islam, M.M., Afrin, S., Ahmed, T., and Ali, M.A.: Meteorological and seasonal
706 influences in ambient air quality parameters of Dhaka city. *J. Civ. Eng.*, 43, 67-77,
707 2015.

708 Jiang, Y., Xing, J., Wang, S., Chang, X., Liu, S., Shi, A., Liu, B., and Sahu, S. K.:
709 Understand the local and regional contributions on air pollution from the view of
710 human health impacts. *Frontiers of Environmental Science and Engineering*,
711 15(5), <https://doi.org/10.1007/s11783-020-1382-2>, 2021.

712 Kitagawa, Y. K. L., Pedruzzi, R., Galvão, E. S., de Araujo, I. B., Albuquerque, T.T.A.,
713 Kumar, P., Nascimento, E. G. S., and Moreira, D. M.: Source apportionment
714 modeling of PM_{2.5} using CMAQ-ISAM over a tropical coastal-urban area. *Atmos.*
715 *Pollut. Res.*, 12, <https://doi.org/10.1016/j.apr.2021.101250>, 2021.

716 Kitagawa, Y. K. L., Kumar, P., Galvão, E. S., Santos, J. M., Reis, N. C., Nascimento, E.
717 G. S., and Moreira, D. M.: Exposure and dose assessment of school children to
718 air pollutants in a tropical coastal-urban area. *Science of the Total Environment*,
719 803, <https://doi.org/10.1016/j.scitotenv.2021.149747>, 2022.

720 Kota, S.H., Zhang, H., Chen, G., Schade, G.W., and Ying, Q.: Evaluation of on-road
721 vehicle CO and NO_x National Emission Inventories using an urban-scale source-
722 oriented air quality model. *Atmos. Environ.* 85, 99-108, 2014.

723 Kota, S.H., Guo, H., Myllyvirta, L., Hu, J., Sahu, S.K., Garaga, R., Ying, Q., Gao, A.,
724 Dahiya, S., Wang, Y., and Zhang, H.: Year-long simulation of gaseous and
725 particulate air pollutants in India. *Atmos. Environ.* 180, 244-255, 2018.

726 Kumar, R., He, C., Bhardwaj, P., Lacey, F., Buchholz, R. R., Brasseur, G. P., Joubert, W.,
727 Labuschagne, C., Kozlova, E., and Mkololo, T: Assessment of regional carbon
728 monoxide simulations over Africa and insights into source attribution and
729 regional transport. *Atmos. Environ.* 119075,
730 <https://doi.org/10.1016/j.atmosenv.2022.119075>, 2022.

731 Kwok, R. H. F., Napelenok, S. L., and Baker, K. R.: Implementation and evaluation of
732 PM_{2.5} source contribution analysis in a photochemical model. *Atmos.*
733 *Environ.* 80, 398-407, <https://doi.org/10.1016/j.atmosenv.2013.08.017>, 2013.

734 Lang, J.L., Liang, X., Li, S., Zhou, Y., Chen, D., Zhang, Y., and Xu, L.: Understanding
735 the impact of vehicular emissions on air pollution from the perspective of regional
736 transport: A case study of the Beijing-Tianjin-Hebei region in China. *Science of*
737 *the Total Environment*, 785, <https://doi.org/10.1016/j.scitotenv.2021.147304>, 2021.

738 Li, M., Song, Y., Huang, X., Li, J., Mao, Y., Zhu, T., Cai, X., and Liu, B.: Improving
739 mesoscale modeling using satellite-derived land surface parameters in the pearl
740 river delta region, China. *Journal of Geophysical Research*, 119(11), 6325–6346,
741 <https://doi.org/10.1002/2014JD021871>, 2014.

742 Li, M., Zhang, Z., Yao, Q., Wang, T., Xie, M., Li, S., Zhuang, B., and Han, Y.:
743 Nonlinear responses of particulate nitrate to NO_x emission controls in the
744 megalopolises of China. *Atmospheric Chemistry and Physics*, 21(19), 15135–
745 15152, <https://doi.org/10.5194/acp-21-15135-2021>, 2021.

746 Li, X., Huang, L., Li, J., Shi, Z., Wang, Y., Zhang, H., Ying, Q., Yu, X., Liao, H., and Hu,
747 J.: Source contributions to poor atmospheric visibility in China. *Resources,*
748 *Conservation & Recycling*, 143, 167-177, 2019.

749 Liu, J., Mauzerall, D. L., Chen, Q., Zhang, Q., Song, Y., Peng, W., Klimont, Z., Qiu, X.
750 H., Zhang, S. Q., Hu, M., Lin, W. L., Smith, K. R., and Zhu, T.: Air pollutant
751 emissions from Chinese households: A major and underappreciated ambient
752 pollution source. *P. Natl. Acad. Sci. USA*, 113, 7756-7761, 2016.

753 Ma, J., Shen, J., Wang, P., Zhu, S., Wang, Y., Wang, P., Wang, G., Chen, J., and Zhang,
754 H.: Modeled changes in source contributions of particulate matter during the
755 COVID-19 pandemic in the Yangtze River Delta, China. *Atmospheric Chemistry*
756 *and Physics*, 21(9), 7343-7355, <https://doi.org/10.5194/acp-21-7343-2021>, 2021.

757 Mao, J., Li, L., Li, J., Sulaymon, I.D., Xiong, K., Wang, K., Zhu, J., Chen, G., Ye, F.,
758 Zhang, N., Qin, Y., Qin, M., and Hu, J.: Evaluation of long-term modeling fine
759 particulate matter and ozone in China during 2013-2019. *Front. Environ. Sci.*
760 10:872249, 10.3389/fenvs.2022.872249, 2022.

761 Marais, E. A., Jacob, D. J., Wecht, K., Lerot, C., Zhang, L., Yu, K., Kurosu, T. P.,
762 Chance, K., and Sauvage, B.: Anthropogenic emissions in Nigeria and implications
763 for atmospheric ozone pollution: A view from space. *Atmos. Environ.*, 99, 32-40,
764 <https://doi.org/10.1016/j.atmosenv.2014.09.055>, 2014.

765 Marais, E. A., Silvern, R. F., Vodonos, A., Dupin, E., Bockarie, A. S., Mickley, L. J.,
766 and Schwartz, J.: Air Quality and Health Impact of Future Fossil Fuel Use for
767 Electricity Generation and Transport in Africa. *Environmental Science and*
768 *Technology*, 53(22), 13524–13534, <https://doi.org/10.1021/acs.est.9b04958>, 2019.

769 Marrapu, P., Cheng, Y., Beig, G., Sahu, S., Srinivas, R., and Carmichael, G.R.: Air
770 quality in Delhi during the Commonwealth games. *Atmos. Chem. Phys.* 14,
771 10619- 10630, 2014.

772 Mazzeo, A., Burrow, M., Quinn, A., Marais, E.A., Singh, A., Nganga, D., Gichuru, M.J.,
773 and Pope, F.D.: Evaluation of the WRF and CHIMERE models for the
774 simulation of PM_{2.5} in large East African urban conurbations. *Atmospheric*
775 *Chemistry and Physics*, 22, 10677-10701, 10.5194/acp-22-10677-2022, 2022.

776 Nedbor-Gross, R., Henderson, B.H., Perez-Pena, M.P., and Pachon, J.E.: Air quality
777 modeling in Bogota Colombia using local emissions and natural mitigation factor
778 adjustment for re-suspended particulate matter. *Atmos. Pollut. Res.* 9, 95-104,
779 <https://doi.org/10.1016/j.apr.2017.07.004>, 2018.

780 Okimiji, O. P., Techato, K., Simon, J. N., Tope-Ajayi, O. O., Okafor, A. T., Aborisade,
781 M. A., and Phoungthong, K.: Spatial pattern of air pollutant concentrations and their
782 relationship with meteorological parameters in coastal slum settlements of Lagos,
783 Southwestern Nigeria. *Atmosphere*, 12(11),
784 <https://doi.org/10.3390/atmos12111426>, 2021.

785 Owoade, O. K., Fawole, O. G., Olise, F. S., Ogundele, L. T., Olaniyi, H. B., Almeida, M.
786 S., Ho, M. D., and Hopke, P. K.: Characterization and source identification of
787 airborne particulate loadings at receptor site-classes of Lagos Mega-City, Nigeria.
788 *Journal of the Air and Waste Management Association*, 63(9), 1026–1035,
789 <https://doi.org/10.1080/10962247.2013.793627>, 2013.

790 Owoade, O.K., Abiodun, P.O., Omokungbe, O.R., Fawole, O.G., Olise, F.S., Popoola,
791 O.O.M., Jones, R.L., and Hopke, P.K.: Spatial-temporal Variation and Local

792 Source Identification of Air Pollutants in a Semi-urban Settlement in Nigeria
793 Using Low-cost Sensors. *Aerosol Air Qual. Res.* 21, 200598,
794 <https://doi.org/10.4209/aaqr.200598>, 2021.

795 Pan, S., Choi, Y., Roy, A., and Jeon, W.: Allocating emissions to 4 km and 1 km
796 horizontal spatial resolutions and its impact on simulated NO_x and O₃ in Houston,
797 TX. *Atmos. Environ.*, 164, 398-415,
798 <https://doi.org/10.1016/j.atmosenv.2017.06.026>, 2017.

799 Pedruzzi, R., Baek, B. H., Henderson, B. H., Aravanis, N., Pinto, J. A., Araujo, I. B.,
800 Nascimento, E. G. S., Reis Junior, N. C., Moreira, D. M., and de Almeida
801 Albuquerque, T. T.: Performance evaluation of a photochemical model using
802 different boundary conditions over the urban and industrialized metropolitan
803 area of Vitória, Brazil. *Environmental Science and Pollution Research*, 26(16),
804 16125–16144, <https://doi.org/10.1007/s11356-019-04953-1>, 2019.

805 Pedruzzi, R., Andreão, W. L., Baek, B. H., Hudke, A. P., Glotfelty, T. W., Dias de Freitas,
806 E., Martins, J. A., Bowden, J. H., Pinto, J. A., Alonso, M. F., and de Almeida
807 Albuquerque, T.T: Update of land use/land cover and soil texture for Brazil:
808 Impact on WRF modeling results over São Paulo. *Atmos. Environ.*, 268, 118760,
809 <https://doi.org/10.1016/j.atmosenv.2021.118760>, 2022.

810 Qiao, X., Tang, Y., Hu, J., Zhang, S., Li, J., Kota, S. H., Wu, L., Gao, H., Zhang, H., and
811 Ying, Q.: Modeling dry and wet deposition of sulfate, nitrate, and ammonium
812 ions in Jiuzhaigou National Nature Reserve, China using a source-oriented CMAQ
813 model: Part I. Base case model results. *Sci. Total Environ.*, 532: 831-839, 2015.

814 Qiao, X., Guo, H., Tang, Y., Wang, P., Deng, W., Zhao, X., Hu, J., Ying, Q., and Zhang,
815 H.: Local and regional contributions to fine particulate matter in the 18 cities
816 of Sichuan Basin, southwestern China. *Atmospheric Chemistry and Physics*, 19(9),
817 5791-5803, <https://doi.org/10.5194/acp-19-5791-2019>, 2019.

818 Reis, S., Liška, T., Vieno, M., Carnell, E.J., Beck, R., Clemens, T., Dragosits, U.,
819 Tomlinson, S.J., Leaver, D., and Heal, M.R.: The influence of residential and
820 workday population mobility on exposure to air pollution in the UK. *Environ. Int.*
821 121, 803-813, <https://doi.org/10.1016/j.envint.2018.10.005>, 2018.

822 Rizwan, S. A., Nongkynrih, B., and Gupta, S. K.: Air pollution in Delhi: its magnitude
823 and effects on health. *Indian journal of community medicine: official publication*
824 *of Indian Association of Preventive & Social Medicine*, 38(1), 4, 2013.

825 Shen, J., Zhao, Q., Cheng, Z., Huo, J., Zhu, W., Zhang, Y., Duan, Y., Wang, X., Antony
826 Chen, L. W., and Fu, Q.: Evolution of source contributions during heavy fine
827 particulate matter (PM_{2.5}) pollution episodes in eastern China through online
828 measurements. *Atmos. Environ.*, 232,
829 <https://doi.org/10.1016/j.atmosenv.2020.117569>, 2020.

830 Shi, Z., Li, J., Huang, L., Wang, P., Wu, L., Ying, Q., Zhang, H., Lu, L., Liu, X., Liao, H.,
831 and Hu, J.: Source apportionment of fine particulate matter in China in 2013
832 using a source-oriented chemical transport model. *Science of the Total*
833 *Environment*, 601-602, 1476-1487,
834 <https://doi.org/10.1016/j.scitotenv.2017.06.019>, 2017.

835 Sulaymon, I. D., Mei, X., Yang, S., Chen, S., Zhang, Y., Hopke, P. K., Schauer, J. J., and
836 Zhang, Y.: PM_{2.5} in Abuja, Nigeria: Chemical characterization, source
837 apportionment, temporal variations, transport pathways and the health risks

838 assessment. Atmospheric Research, 237,
839 <https://doi.org/10.1016/j.atmosres.2019.104833>, 2020.

840 Sulaymon, I. D., Zhang, Y., Hopke, P. K., Hu, J., Zhang, Y., Li, L., Mei, X., Gong, K.,
841 Shi, Z., Zhao, B., and Zhao, F.: Persistent high PM_{2.5} pollution driven by
842 unfavorable meteorological conditions during the COVID-19 lockdown period in
843 the Beijing-Tianjin-Hebei region, China. Environmental Research, 198.
844 <https://doi.org/10.1016/j.envres.2021.111186>, 2021a.

845 Sulaymon, I. D., Zhang, Y., Hu, J., Hopke, P. K., Zhang, Y., Zhao, B., Xing, J., Li, L.,
846 and Mei, X.: Evaluation of regional transport of PM_{2.5} during severe atmospheric
847 pollution episodes in the western Yangtze River Delta, China. Journal of
848 Environmental Management, 293, <https://doi.org/10.1016/j.jenvman.2021.112827>,
849 2021b.

850 Sulaymon, I. D., Zhang, Y., Hopke, P. K., Zhang, Y., Hua, J., and Mei, X.: COVID-
851 19 pandemic in Wuhan: Ambient air quality and the relationships between criteria
852 air pollutants and meteorological variables before, during, and after lockdown.
853 Atmospheric Research, 250, <https://doi.org/10.1016/j.atmosres.2020.105362>,
854 2021c.

855 Sulaymon, I. D., Zhang, Y., Hopke, P. K., Hu, J., Rupakheti, D., Xie, X., Zhang, Y.,
856 Ajibade, F. O., Hua, J., and She, Y.: Influence of transboundary air pollution
857 and meteorology on air quality in three major cities of Anhui Province, China.
858 Journal of Cleaner Production, 129641,
859 <https://doi.org/10.1016/j.jclepro.2021.129641>, 2021d.

860 Tao, H., Xing, J., Zhou, H., Pleim, J., Ran, L., Chang, X., Wang, S., Chen, F., Zheng, H.,
861 and Li, J.: Impacts of improved modeling resolution on the simulation of
862 meteorology, air quality, and human exposure to PM_{2.5}, O₃ in Beijing, China.
863 Journal of Cleaner Production, 243, <https://doi.org/10.1016/j.jclepro.2019.118574>,
864 2020.

865 Tiwari, S., Thomas, A., Rao, P., Chate, D. M., Soni, V. K., Singh, S., Ghude, S. D., Singh,
866 D., and Hopke, P. K.: Pollution concentrations in Delhi India during winter
867 2015-2016: A case study of an odd-even vehicle strategy. Atmos. Pollut. Res., 9,
868 1137-1145, 2019.

869 Wang, P., Ying, Q., Zhang, H., Hu, J., Lin, Y., and Mao, H.: Source apportionment of
870 secondary organic aerosol in China using a regional source-oriented chemical
871 transport model and two emission inventories. Environmental Pollution, 237, 756-
872 766, <https://doi.org/10.1016/j.envpol.2017.10.122>, 2018.

873 Wang, P., Chen, K., Zhu, S., Wang, P., and Zhang, H.: Severe air pollution events not
874 avoided by reduced anthropogenic activities during COVID-19 outbreak.
875 Resources, Conservation and Recycling, 158,
876 <https://doi.org/10.1016/j.resconrec.2020.104814>, 2020.

877 Wang, P., Wang, P., Chen, K., Du, J., and Zhang, H.: Ground-level ozone simulation
878 using ensemble WRF/Chem predictions over the Southeast United States.
879 Chemosphere, 287, <https://doi.org/10.1016/j.chemosphere.2021.132428>, 2021a.

880 Wang, X., Li, L., Gong, K., Mao, J., Hu, J., Li, J., Liu, Z., Liao, H., Qiu, W., Yu, Y.,
881 Dong, H., Guo, S., Hu, M., Zeng, L., and Zhang, Y.: Modelling air quality during the
882 EXPLORE-YRD campaign - Part I. Model performance evaluation and impacts

883 of meteorological inputs and grid resolutions. *Atmos. Environ.*, 246,
884 <https://doi.org/10.1016/j.atmosenv.2020.118131>, 2021b.

885 WHO. WHO Air Quality Guidelines Global Update.: Particulate Matter, Ozone,
886 Nitrogen Dioxide and Sulphur Dioxide; World Health Organization Regional
887 Office for Europe. World Health Organization, Copenhagen, Denmark, 2005.

888 Wiedinmyer, C., Akagi, S., Yokelson, R. J., Emmons, L., Al-Saadi, J., Orlando, J., and
889 Soja, A.: The Fire INventory from NCAR (FINN): A high resolution global
890 model to estimate the emissions from open burning. *Geoscientific Model Devel.*,
891 4 (3), 625, 2011.

892 World Health Organization.: WHO Global Air Quality Guidelines: Particulate Matter
893 (PM_{2.5} and PM₁₀), Ozone, Nitrogen Dioxide, Sulfur Dioxide and Carbon
894 Monoxide. World Health Organization. Available at:
895 <https://apps.who.int/iris/handle/10665/345329>, 2021.

896 Yan, D., Lei, Y., Shi, Y., Zhu, Q., Li, L., and Zhang, Z.: Evolution of the spatiotemporal
897 pattern of PM_{2.5} concentrations in China - A case study from the Beijing-Tianjin-
898 Hebei region. *Atmos. Environ.*, 183, 225–233,
899 <https://doi.org/10.1016/j.atmosenv.2018.03.041>, 2018.

900 Ye, F., Rupakheti, D., Huang, L., T, Nishanth., MK, S.K., Li, L., KT, V., Hu, J.: Integrated
901 process analysis retrieval of changes in ground-level ozone and fine particulate
902 matter during the COVID-19 outbreak in the coastal city of Kannur, India.
903 *Environmental Pollution*, 307, <https://doi.org/10.1016/j.envpol.2022.119468>,
904 2022.

905 Ying, Q. and Kleeman, M.J.: Source contributions to the regional distribution of
906 secondary particulate matter in California. *Atmos. Environ.*, 40, 736-752, 2006.

907 Ying, Q., Wu, L., and Zhang, H.: Local and inter-regional contributions to PM_{2.5}
908 nitrate and sulfate in China. *Atmos. Environ.*, 94, 582-592, 2014.

909 Ying, Q., Li, J., and Kota, S.H.: Significant contributions of isoprene to summertime
910 secondary organic aerosol in eastern United States. *Environ. Sci. Technol.*, 49,
911 7834-7842, 2015.

912 Yu, Y., Xu, H., Jiang, Y., Chen, F., Cui, X., He, J., and Liu, D.: A modeling study of
913 PM_{2.5} transboundary during a winter severe haze episode in southern Yangtze
914 River Delta, China. *Atmos. Res.*, 248, 105159, 2021.

915 Zhang, H., Li, J., Ying, Q., Guven, B.B., and Olaguer, E.P.: Source apportionment
916 of formaldehyde during TexAQS 2006 using a source-oriented chemical
917 transport model. *J. Geophys. Res. Atmos.*, 118, 1525-1535, 2013.

918 Zhang, H., Hu, J., Kleeman, M., and Ying, Q.: Source apportionment of sulfate and
919 nitrate particulate matter in the Eastern United States and effectiveness of
920 emission control programs. *Sci. Total Environ.* 490, 171-181, 2014.

921 Zhang, H., Wang, Y., Hu, J., Ying, Q., and Hu, X.: Relationships between
922 meteorological parameters and criteria air pollutants in three megacities in
923 China. *Environ. Res.*, 140, 242-254, 2015.

924 Zhang, H., Cheng, S., Yao, S., Wang, X., and Zhang, J.: Multiple perspectives for
925 modeling regional PM_{2.5} transport across cities in the Beijing-Tianjin-Hebei
926 region during haze episodes. *Atmos. Environ.*, 212, 22-35, 2019.

927 Zhang, Q., Ma, Q., Zhao, B., Liu, X., Wang, Y., Jia, B., and Zhang, X.: Winter haze
928 over North China Plain from 2009 to 2016: Influence of emission and

929 meteorology. Environmental Pollution,
930 <https://doi.org/10.1016/j.envpol.2018.08.019>, 2018.
931 Zhao, X., Wang, G., Wang, S., Zhao, N., Zhang, M., and Yue, W.: Impacts of
932 COVID-19 on air quality in mid-eastern China: An insight into meteorology
933 and emissions. Atmos. Environ., 266,
934 <https://doi.org/10.1016/j.atmosenv.2021.118750>, 2021.